REPORTS

Transplacental Effects of 3′-Azido-2′,3′-Dideoxythymidine (AZT): Tumorigenicity in Mice and Genotoxicity in Mice and Monkeys

*Ofelia A. Olivero, Lucy M. Anderson, Bhalchandra A. Diwan, Diana C. Haines, Steven W. Harbaugh, Thomas J. Moskal, Ann B. Jones, Jerry M. Rice, Charles W. Riggs, Daniel Logsdon, Stuart H. Yuspa, Miriam C. Poirier**

Background: **When given during pregnancy, the drug 3′-azido-2′,3′-dideoxythymidine (AZT) substantially reduces maternal–fetal transmission of human immunodeficiency virus type 1 (HIV-1). However, AZT has been shown to be carcinogenic in adult mice after lifetime oral administration. In this study, we assessed the transplacental tumorigenic and genotoxic effects of AZT in the offspring of CD-1 mice and *Erythrocebus patas* monkeys given AZT orally during pregnancy. *Methods:* Pregnant mice were given daily doses of either 12.5 or 25.0 mg AZT on days 12 through 18 of gestation (last 37% of gestation period). Pregnant monkeys were given a daily dose of 10.0 mg AZT 5 days a week for the last 9.5–10 weeks of gestation (final 41%–43% of gestation period). AZT incorporation into nuclear and mitochondrial DNA and the length of chromosomal end (telomere) DNA were examined in multiple tissues of newborn mice and fetal monkeys. Additional mice were followed from birth and received no further treatment until subjected to necropsy and complete pathologic examination at 1 year of age. An anti-AZT radioimmunoassay was used to monitor AZT incorporation into DNA. *Results:* At 1 year of age, the offspring of AZT-treated mice exhibited statistically significant, dose-dependent increases in tumor incidence and tumor multiplicity in the lungs, liver, and female reproductive organs. AZT incorporation into nuclear and mitochondrial DNA was detected in multiple organs of transplacentally exposed mice and monkeys. Shorter chromosomal telomeres were detected in liver and brain tissues from most AZT-exposed newborn mice but not in tissues from fetal monkeys. *Conclusions:* AZT is genotoxic in fetal mice and monkeys and is a moderately strong transplacental carcinogen in mice examined at 1 year of age. Careful long-term follow-up of AZT-exposed children would seem to be appropriate.** **[J Natl Cancer Inst 1997;89:1602–8]**

Exposure of pregnant females of numerous mammalian species, including nonhuman primates, to various chemical carcinogens results in neoplasms in their offspring *(1)*. The human relevance of transplacental carcinogenesis was established with the discovery that diethylstilbestrol (DES) caused vaginal adenocarcinomas in the children of women treated during pregnancy *(2)*. Subsequent experimental studies in mice duplicated this effect *(3)*. Epidemiologic evidence has implicated transplacental exposures to radiation, certain medications, pesticides, occupational chemicals, and metals *(4–6)* as possible contributors to human cancer risk. Mechanistic studies with rodents indicate that fetuses may be particularly at risk of tumor initiation by chemicals, with high rates of cell division and other fetal characteristics greatly enhancing vulnerability *(7)*.

The nucleoside analogue 3′-azido-2′,3′-dideoxythymidine (AZT), widely used to treat human immunodeficiency virus type 1 (HIV-1) infection, has become the standard of care in preventing fetal transmission of the virus in HIV-1-positive pregnant women *(8,9)*. Recommended treatment encompasses five daily 100.0-mg doses (approximately 8.3 mg/kg body weight per day) during the second and third trimesters of pregnancy, with additional maternal intravenous dosing at delivery and oral AZT given to the infant after birth *(9,10)*. In a recent study from the Pediatric AIDS (i.e., acquired immunodeficiency syndrome) Clinical Trials Group *(9)*, this regimen reduced viral transmission to the fetus from 22.6% (n = 204) to 7.6% (n = 198).

In adult mice, AZT is carcinogenic. Ayers et al. *(11)* reported 10% and the National Toxicology Program *(12)* reported 22% incidences of vaginal squamous papillomas and carcinomas after lifetime oral administration of the drug to CD-1 and $B6C3F_1$ mice, respectively. At similar doses in mice exposed to AZT for 28 days, dose-related incorporation of AZT into vaginal DNA and increased vaginal epithelial proliferation were observed *(13)*. Because of the projected widespread use of AZT in human pregnancy, we have investigated the genotoxic and carcinogenic effects of AZT in the

**Affiliations of authors:* O. A. Olivero, S. H. Yuspa, M. C. Poirier, Laboratory of Cellular Carcinogenesis and Tumor Promotion, Division of Basic Sciences, National Cancer Institute, Bethesda, MD; L. M. Anderson, A. B. Jones, Laboratory of Comparative Carcinogenesis, Division of Basic Sciences, National Cancer Institute, National Cancer Institute-Frederick Cancer Research and Development Center, Frederick, MD; B. A. Diwan (Intramural Research Supported Program), D. C. Haines (Pathology/Histotechnology Laboratory), D. Logsdon (Laboratory Animal Sciences Program), Science Applications International Corp.–National Cancer Institute-Frederick Cancer Research and Development Center; S. W. Harbaugh, T. J. Moskal, BioQual, Inc., Rockville, MD; J. M. Rice, International Agency for Research on Cancer, Lyon, France; C. W. Riggs, Data Management Services, Inc., National Cancer Institute-Frederick Cancer Research and Development Center.

Correspondence to: Ofelia A. Olivero, Ph.D., National Institutes of Health, Bldg. 37, Rm. 3B15, MSC-4255, Bethesda, MD 20892–4255. E-mail: olivero@pop.nci.nih.gov

See ''Notes'' following ''References.''

offspring of exposed pregnant CD-1 mice and AZT genotoxicity in the fetuses of exposed pregnant *Erythrocebus patas* monkeys.

Materials and Methods

Source and Purity of AZT

AZT (lot No. 063H7819) was obtained from Sigma Chemical Co., St. Louis, MO. The purity of AZT was assessed by means of elemental analysis, UV spectrum analysis, nuclear magnetic resonance spectrometry, and mass spectrometry, as well as by means of high-performance liquid chromatography with two different mobile phases (data not shown). All of the parameters were consistent with literature values, confirming the AZT structure and assessing the purity of this lot at greater than 99.8%. The determinations were performed by Dr. Haleem J. Issaq of the Chemical Synthesis and Analysis Laboratory, Science Applications International Corp. (SAIC), National Cancer Institute (NCI)-Frederick Cancer Research and Development Center (FCRDC), Frederick, MD.

Tumorigenicity in the Offspring of Pregnant Mice Receiving AZT

Animal care for this experiment was provided in accordance with the procedures outlined in the *Guide for the Care and Use of Laboratory Animals* [National Institutes of Health publication No. (NIH)86–23, 1985] under an animal study proposal approved by the FCRDC Animal Care and Use Committee. Female CD-1 Swiss mice (Charles River, Raleigh, NC) were given food and water *ad libitum.* The mice were mated, and day 1 of pregnancy was ascertained by the presence of a vaginal plug. Forty-five pregnant mice were given 0 (17 litters), 12.5 (13 litters), or 25.0 (15 litters) mg AZT in 0.5 mL sterile distilled water via an intragastric tube once daily on days 12 through 18 of gestation. Preliminary toxicity studies indicated that the maximum fetal-tolerated daily dose was 25.0 mg (approximately 420 mg/kg term body weight), with doses of 30.0–50.0 mg causing fetal or newborn loss. The pups were delivered normally. The average number of pups weaned per litter was 11.7, 12.1, and 10.1 for the control, low-dose, and high-dose groups, respectively. Ten mice per sex from each group of pups were killed on schedule at 13, 26, and 52 weeks after delivery. No tumors were evident at the first two time points. However, at 52 weeks, lung and liver tumors were observed in the AZT-exposed mice, so additional animals (selected at random) were killed to obtain numbers adequate for statistical analysis. In addition, moribund mice from all groups were killed, and the findings from these mice were included with the findings from the mice killed at 52 weeks. Altogether, the numbers of litters represented were five (61 mice) for the control group (i.e., no AZT), six (45 mice) for the 12.5-mg-AZT group, and nine (50 mice) for the 25.0-mg-AZT group. All remaining mice will be killed at 2 years of age.

When moribund or at planned sacrifice, mice underwent a complete necropsy. Lungs, liver, ovary/testis, uterus/cervix/vagina, thymus, spleen, lymph nodes, kidneys, brain, pituitary, mammary gland, femur, cecum, and all grossly noted lesions and masses were examined by means of light microscopy. The pathology findings were peer-reviewed by Dr. Miriam Anver, SAIC, NCI-FCRDC, and by Dr. Jerrold Ward, Office of Laboratory of Animal Sciences, NCI. All lung, liver, and female reproductive tract lesions were reviewed, as well as all questionable and representative definitive hematopoietic lesions. Spiral organisms, thought to be *Helicobacter hepaticus,* were observed in Steiner's stained slides of most ceca, but only a few organisms were observed in one liver, and no hepatitis was observed in any of the livers. The mice were otherwise specific pathogen free. Tumor data are presented as tumor incidence (percent of animals with tumors) and tumor multiplicity (number of tumors per animal).

Statistical Methods

Dose-dependent linear trends of tumor incidence proportions were evaluated by use of the Cochran–Armitage chi-squared test (two-tailed) *(14),* and high-dose versus control comparisons were made by use of Fisher's exact test (two-tailed) *(15).* Two-tailed chi-squared tests *(16)* were used to analyze the reduction in hematopoietic neoplasms in AZT-exposed males and females in relationship to control animals. Tests of the homogeneity of the proportions of tumor bearers per litter within each of the sex–dose–organ groups were performed by use of the correlated binomial $C(\alpha)$ test statistic as described by Tarone *(17).* In addition, for lungs and liver, comparisons of low-dose treatment with high-dose treatment on the basis of litters involved the analysis of variance of 1) raw proportions of tumor-bearing animals in each litter and 2) Freeman–Tukey arcsine transformations of the proportions *(18),* with each analysis using weights proportional to the litter sizes. Tumor multiplicities were tested for dose-dependent trends by use of the nonparametric Jonckheere test (two-tailed) *(19),* and high-dose versus control comparisons were made by use of the nonparametric Wilcoxon rank-sum test (two-tailed) *(20).*

Incorporation of AZT Into Nuclear and Mitochondrial DNA of Fetal CD-1 Mice Exposed *In Utero* to AZT

Pregnant CD-1 mice were given 0 (n = 3) or 25.0 (n = 3) mg AZT/day by gavage on days 12 through 18 of gestation (final 37% of gestation period), and the pups (14 each for litters 1 and 3 and 11 for litter 2) were born 24 hours or less after the last exposure. For each organ (e.g., kidneys), tissue from all of the pups of one litter was combined. The samples were homogenized, and DNA was isolated by means of the Oncor nonorganic extraction method (Oncor, Inc., Gaithersburg, MD). Mitochondrial DNA was prepared as previously described *(21).*

DNA samples, in distilled water, were sonicated for 30 seconds and then boiled for 5 minutes. Three-microgram aliquots of DNA were subsequently assayed by use of a competitive anti-AZT radioimmunoassay (AZT-RIA) as previously described *(22).* Briefly, a rabbit polyclonal anti-AZT antibody (Sigma Chemical Co.) that also recognizes AZT in DNA was reconstituted in 20 mL 10 m*M* Tris buffer (pH 8.0), representing a 1:5000 dilution of the antibody. A 0.1-mL aliquot of the diluted antibody was incubated in a 12 × 75-mm disposable glass tube with an equal volume of a solution containing either standard AZT plus 3 μg calf thymus carrier DNA (Sigma Chemical Co.) or a 3-μg sample of DNA from AZT-treated or untreated (control) animals for 90 minutes at 37 °C. Approximately 20 000 cpm [^{3}H]AZT tracer (20 Ci/mmol; Moravek Biochemicals, Inc., Mountain View, CA), in a volume of 100 μL, was added per tube together with 100 μL goat anti-rabbit immunoglobulin G secondary antibody (ICN Biomedicals, Inc., Costa Mesa, CA; reconstituted in 12 mL 10 m*M* Tris buffer [pH 8.0]), and the mixture was incubated for 25 minutes at 4 °C. The mixture was centrifuged at 2000*g* for 15 minutes at 4 °C. The resulting supernatant was decanted, and the pellets were dissolved in 100 m*M* NaOH and counted in a liquid scintillation counter.

The AZT-RIA employs a radiolabeled AZT tracer, used in a constant amount in each tube, to compete with the AZT standard, used at different concentrations, or sample DNA for binding to the anti-AZT antibody. In the absence of standard AZT or sample DNA containing AZT, the highest level of radiolabel binding to the antibody will be obtained (cpm with no inhibitor). Because of the competitive nature of this assay, the added presence of nonradiolabeled AZT (i.e., the standard or in the sample DNA) will result in the inhibition of tracer-antibody binding (cpm with inhibitor). The inhibition of tracer-antibody binding observed with a particular amount (''x'') of unlabeled AZT is expressed as a percent according to the following formula:

$$\text{Percent inhibition} = \frac{[(\text{cpm with no inhibitor}) - (\text{cpm with amount ''x'' of inhibitor})]}{(\text{cpm with no inhibitor})} \times 100.$$

The amount of standard AZT added to 3 μg carrier calf thymus DNA that inhibited antibody binding by 50% was 570 ± 420 fmol (mean ± standard deviation [SD]; n = 12) for the mouse assays. The amount of AZT in 3 μg of biologic sample DNA was obtained by comparing DNA from the corresponding tissue of an untreated animal with DNA from a treated animal, calculating the percent inhibition of antibody binding, and reading the amount of AZT from a plotted standard curve. Each sample was assayed in three to five separate radioimmunoassays.

Incorporation of AZT Into Fetal *Erythrocebus patas* Monkey Nuclear and Mitochondrial DNA

Monkeys were maintained and treated under American Association for Accreditation of Laboratory Animal Care-approved conditions at BioQual, Inc. (Rockville, MD), in accordance with humane principles for laboratory animal care. Protocols were reviewed and approved by the Animal Care and Use Committee of BioQual, Inc. Pregnancies were ascertained as described *(23).* Pregnant patas monkeys were given 0 (n = 3) or 10.0 (n = 3) mg of AZT/day (approximately 1.5 mg/kg body weight per day) in a piece of banana, 5 days per week for the last 9.5–10 weeks of gestation (final 41%–43% of gestation period). Dose ingestion was confirmed by an observer. Fetuses were taken by cesarean section, performed on the monkeys under Telazol and isofluorane anesthesia, on days 149 through 152 of gestation (24 hours after the last dose). Tissue processing for DNA preparation and the AZT-RIA were as

described above for newborn mouse tissues, except that the 50% inhibition value for the RIA was 820 ± 290 fmol AZT (mean ± SD; n = 25).

Examination of Telomere Length in Mouse and Monkey Tissues

The length of telomeric (chromosomal end) DNA *(24)* was examined in DNA from the tissues of 10 newborn mouse litters, either unexposed (n = 5) or exposed (n = 5) *in utero* to 25.0 mg AZT/day on days 12 through 18 of gestation. For each litter, tissues from different organs were combined and homogenized with a Dounce homogenizer, and high-molecular-weight DNA was prepared by use of the nonorganic extraction method of Oncor, Inc. The DNA was digested with *Alu* I, *Rsa* I, and *Sau* 3A I restriction endonucleases (New England Biolabs, Inc., Beverly, MA) and resolved in 1% agarose gels along with biotinylated molecular markers (Oncor, Inc.). The DNA was transferred to nylon support membranes overnight by means of capillary action *(25)*, and it was cross-linked to the membranes by use of UV light. The membranes were blocked for 30 minutes at 45 °C with blocking solution (Oncor, Inc.) and hybridized with a biotinylated human telomeric repeat sequence probe (Oncor, Inc.) overnight in a sealed bag at 45 °C. Posthybridization washes were performed in a solution of 0.16× standard saline citrate and 0.1% sodium dodecyl sulfate for 1 hour at 60 °C. The membranes were subsequently blocked with a 5% low-fat milk solution at room temperature for 30 minutes, and an amplified alkaline phosphatase immunoblot assay kit (Biorad Laboratories, Hercules, CA) was used in membrane staining. The sizes of the telomere repeats were determined by comparison with the biotinylated molecular markers. A similar approach was used to examine telomere length in DNA from the tissues of six fetal monkeys exposed to either 0 (n = 3) or 10.0 mg AZT/day for the last 9.5–10 weeks of gestation (n = 3).

Results

Evaluation of AZT as a Transplacental Carcinogen

To test for transplacental tumorigenicity, pregnant CD-1 Swiss dams were exposed once daily to 0, 12.5, or 25.0 mg AZT via intragastric intubation on days 12 through 18 of gestation. In the carcinogenicity study, litter sizes did not differ substantially between AZT-exposed and control mice, and no further exposures were given postnatally. Ten offspring of each sex from each treatment group were necropsied at 3 and 6 months, and no neoplasms were found. However, the interim sacrifice at approximately 1 year revealed the presence of tumors, prompting the sacrifice of additional animals of each sex in each group for further analysis. Complete necropsy and histopathologic analysis of dead, moribund, or sacrificed animals at 190–400 days of age (average ages of 350–382 days) revealed a severalfold, dose-dependent increase in the incidence (Fig. 1) and the multiplicity (Table 1) of tumors in the AZT-exposed groups.

The spontaneous liver and lung adenomas in the control animals are typical for this strain of mice *(26)*. At the same sites, incidences of these types of tumors were increased twofold to eightfold in AZT-treated animals (Fig. 1, A–C). For both sexes combined, the incidence of lung carcinomas increased significantly with AZT dose (3%, 7%, and 14% for the 0-, 12.5-, and 25.0-mg AZT groups, respectively; $P = .037$, two-tailed chi-squared test). Neoplasms of the female organs (ovary, uterus, and vagina) were absent from the control animals but were detected in 14% and 17% of the AZT-exposed female offspring at the low and high doses, respectively (Fig. 1, D).

Neoplasms of the hematopoietic system, including lymphomas, myelogenous leukemia, and histiocytic sarcoma, which occur spontaneously in this mouse strain, were reduced from 33% and 16% in unexposed females and males, respectively, to 8% in the mouse pups of both sexes (Fig. 1, E and F). This reduction suggests that an endogenous oncogenic retrovirus may be inhibited by the AZT treatment and/or that alterations in the immune system may occur in the offspring exposed to AZT *in utero.*

Statistical Analyses for the Tumor Study

Probability values for the tumor incidences presented in Fig. 1 are shown in the legend, and those for the tumor mul-

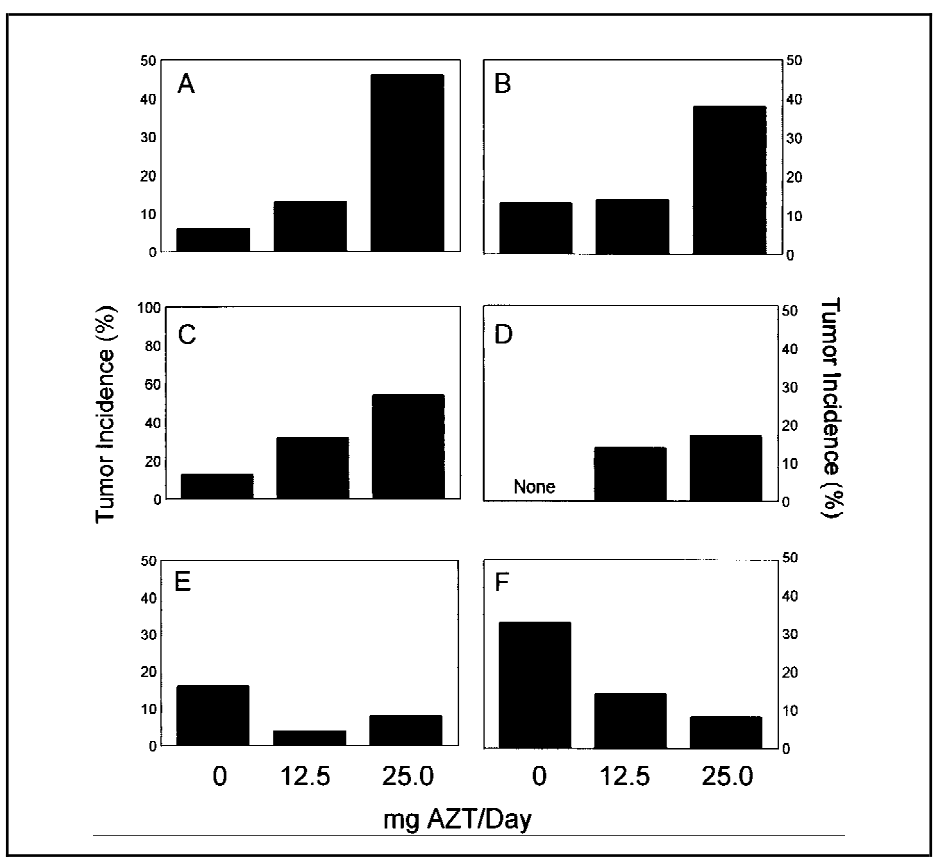

Fig. 1. Tumor incidences in internal organs of offspring of pregnant mice 190–400 days after transplacental 3′-azido-2′,3′-dideoxythymidine (AZT) exposure. Pregnant CD-1 mice were given 0, 12.5, or 25.0 mg AZT in sterile distilled water once daily on days 12 through 18 of gestation. Pups were delivered normally and given no further treatment. When moribund or at sacrifice (190–400 days), the mice underwent complete necropsy (*see* ''Materials and Methods'' section). The figure shows the following tumor incidences: lung tumors (from bronchoalveolar cells) in males (**A**) and in females (**B**); hepatocellular adenomas, including two carcinomas, in males (**C**); female reproductive organ tumors (**D**); and hematopoietic tumors in males (**E**) and females (**F**). Tumor incidences were analyzed for dose-related linear trend by use of the Cochran–Armitage chi-squared test (two-sided). High-dose AZT (25.0 mg AZT) versus control (no AZT) comparisons employed the Fisher's exact test (two-sided). Probability values for these two tests are, respectively, .0004 and .00066 for male lung tumors (**A**); .037 and .056 for female lung tumors (**B**); .0011 and .0014 for male liver tumors (**C**); and .033 and .034 for female reproductive organ tumors (**D**).

tiplicities in Table 1 are shown in a table footnote. The presented statistical relationships are based on pooled groups, since preliminary tests indicated that litter proportions within each test group were generally homogeneous. A possible exception was noted for the male–lung–high-dose group, where near-significant heterogeneity was found ($P = .058$), which was due exclusively to one litter with lung tumors in all five male offspring. Reanalysis of the data excluding this litter resulted in somewhat lower significance probabilities but no overall change in conclusions. When analyzed on a litter basis, comparisons of low- with high-dose AZT for the lungs and the liver produced results that generally reaffirmed the conclusions based on pooled groups.

Transplacental AZT Exposure and Genotoxicity in Newborn Mice and Fetal Monkeys

Using a sensitive anti-AZT radioimmunoassay (AZT-RIA) *(22)* and comparing DNA from exposed and unexposed animals (*see* ''Materials and Methods'' section), we detected AZT incorporation in the nuclear and mitochondrial DNA from multiple pooled organs of newborn CD-1 mouse pups (three litters) after transplacental exposure to 25.0 mg AZT/day on days 12 through 18 of gestation (Table 2, A). Incorporation was widely variable among litters, organs, and DNA compartments, suggesting that undefined pharmacokinetic and specific tissue factors influence persistent AZT incorporation. Litter size appeared to influence measurable incorporation levels, since litters 1 and 3 each consisted of 14 pups and had the lowest incorporation levels, and litter 2, with only 11 pups, had higher incorporation levels.

Telomerase is active in fetal tissues and tumor cells *(27)*, and previous studies have demonstrated that AZT can be preferentially incorporated into the telomeric DNA of cells containing telomerase *(24)*. *In vitro* long-term exposure to 800 μM AZT was shown to produce an irreversible shortening of telomeres *(28)*. In this study, telomere length was examined in five litters of newborn mice exposed to 25.0 mg AZT/day as described in Table 2, A. Fig. 2 shows the results for liver, lungs, and brain from one litter. In comparison with the DNA from control animals, smaller sized telomeric DNA was detected in the livers from five litters, the brains from three of five litters, the lungs from two of five litters, and the kidneys from one of five litters of AZT-treated animals. The variability between litters observed for telomere length is similar to that seen for AZT incorporation into DNA.

The data in mice demonstrated AZT-induced genotoxic and carcinogenic effects at a high dose. To approximate the human exposure of about 8.3 mg/kg body weight per day, we gave three pregnant *Erythrocebus patas* monkeys 10.0 mg AZT/day (approximately 1.5 mg/kg body weight per day) 5 days a week during the last 9.5–10 weeks of a 23-week gestation. Multiple fetal tissues were obtained after cesarean section. AZT incorporation was observed in the nuclear and mitochondrial DNA of transplacentally exposed monkeys but not in the DNA of unexposed control animals (Table 2, B). Even though the monkey dose was much lower than the dose received by the mouse, incorporation levels were generally several-fold higher than those observed in the mouse.

Table 1. Tumor multiplicities at 190–400 days of age in offspring of mice given 0, 12.5, or 25.0 mg 3′-azido-2′,3′-dideoxythymidine (AZT) per day by gavage on days 12 through 18 of gestation*

		Organ of tumorigenesis			
AZT exposure, mg	Offspring evaluated	Lungs, mean No. of tumors ± SE†	Liver, mean No. of tumors ± SE‡	Female organs, No. of tumors	Incidental, No. of tumors
0	31 males	0.10 ± 0.07 (1 CA)	0.23 ± 0.14	na	2 liver hemangiosarcomas
	30 females	0.13 ± 0.06 (1 CA)	0	0	1 skin basal cell tumor
12.5	23 males	0.13 ± 0.07 (1 CA)	0.48 ± 0.18 (1 CA)	na	1 skin papilloma; 1 skin hemangiosarcoma
	22 females	0.14 ± 0.07 (2 CA)	0	2 uterine endometrial stromal polyps; 1 vaginal leiomyosarcoma	None
25.0	26 males	0.50 ± 0.11 (4 CA)	0.79 ± 0.26 (1 CA)	na	None
	24 females	0.38 ± 0.10 (3 CA)	0	1 Sertoli cell tumor, ovary; 1 histiocytic sarcoma, uterus; 1 hemangiosarcoma, uterus; 1 endometrial stromal polyp, uterus	1 skin papilloma; 1 malignant tumor§

*Tumor multiplicity refers to the number of tumors per animal. Results include findings from moribund and dead animals and those killed at 12–13 months. SE = standard error; CA = carcinoma; na = not applicable. *P* values (two-tailed) for trends and comparisons were as follows: Male lung tumors—trend test, $P = .014$; control (0 mg AZT) versus high-dose AZT (25.0 mg), $P = .001$; low-dose AZT (12.5 mg) versus high-dose AZT, $P = .012$. Female lung tumors—trend test, $P = .15$; control versus high-dose AZT, $P = .042$; low-dose AZT versus high-dose AZT, $P = .071$. Male liver tumors—trend test, $P = .013$; control versus high-dose AZT, $P = .0016$; control versus low-dose AZT, $P = .097$. Trend tests were performed with the Jonckheere test, and pairwise treatment comparisons were made by use of the Wilcoxon rank-sum test (both are nonparametric methods).

†Lung alveolar cell adenomas and carcinomas.

‡Liver hepatocellular adenomas.

§Autolyzed neoplasm involving pancreas and spleen.

Table 2, A. Incorporation of 3′-azido-2′,3′-dideoxythymidine (AZT) into nuclear and mitochondrial DNA of fetal CD-1 mice exposed *in utero* to AZT*

	fmol AZT/μg DNA†					
	Litter 1		Litter 2		Litter 3	
Organ	Nuclear	Mt	Nuclear	Mt	Nuclear	Mt
Brain	nd	nd	nd	49.5 ± 3.9‡	nd	nd
Lungs	nd	nd	226.7 ± 128.4	nd	40.3 ± 9.4	51.4 ± 15.0
Liver	nd	nd	121.1 ± 78.9‡	42.9 ± 14.9‡	nd	nd
Kidneys	23.2 ± 2.5	28.4 ± 7.5	41.2 ± 1.2‡	nd	nd	33.3 ± 13.3‡
Skin	nd	160.8 ± 43.6	87.5 ± 23.5‡	302.7 ± 64.0‡	ns	227.0 ± 195.0‡

*Pregnant CD-1 mice were given 0 (n = 3) or 25.0 (n = 3) mg AZT/day, and the pups (14 each for litters 1 and 3 and 11 for litter 2) were born 24 hours or less after the last exposure. For each organ (e.g., kidneys), tissue from all of the pups of one litter was combined, nuclear and mitochondrial DNA was prepared, and 3-μg aliquots of DNA were assayed by use of an anti-AZT radioimmunoassay (*see* ''Materials and Methods'' section). Incorporation is expressed as fmol AZT/μg DNA in relation to results obtained with tissue DNA from unexposed mice. Except where noted, values are means ± standard error for three to five assays.

†Mt = mitochondrial; nd = not detectable; ns = no sample.

‡Mean ± range for samples assayed twice.

Table 2, B. Incorporation of AZT into fetal *Erythrocebus patas* monkey nuclear and mitochondrial DNA*

	fmol AZT/μg DNA†					
	Monkey No. R105		Monkey No. R200		Monkey No. R226	
Organ	Nuclear	Mt	Nuclear	Mt	Nuclear	Mt
Brain	nd	120.0 ± 40.0‡	150.0 ± 70.0‡	nd	nd	242.0 ± 89.4
Cerebellum	227.7 ± 94.7	nd	81.5 ± 11.5‡	ns	252.7 ± 84.0	282.0 ± 54.7
Lungs	739.0 ± 221.1	253.7 ± 135.9	nd	nd	166.7 ± 13.3	203.0 ± 8.8
Liver	566.0 ± 274.0	nd	230.0 ± 70.0‡	55.0 ± 15.0‡	146.0 ± 69.1	nd
Kidneys	703.0 ± 262.6	nd	170.0 ± 30.0‡	55.0 ± 5.0‡	316.6 ± 101.1	nd
Heart	541.6 ± 84.9	155.0 ± 63.7	60.0 ± 10.0‡	45.0 ± 5.0‡	316.0 ± 152.8	324.3 ± 42.4
Placenta	nd	22.0 ± 6.0‡	nd	60.0 ± 0‡	341.7 ± 123.8	nd

*Pregnant patas monkeys were given 0 (n = 3) or 10.0 (n = 3) mg of AZT/day (approximately 1.5 mg/kg body weight per day) in a piece of banana 5 days per week for the last 9.5–10 weeks of gestation. Fetuses were taken by cesarean section on days 149 through 152 of gestation (24 hours after the last dose). Tissue processing and AZT-DNA radioimmunoassay were as described in the ''Materials and Methods'' section, with comparison of DNAs from unexposed and exposed monkeys. Except where noted, values are means ± standard error for three to five assays.

†Mt = mitochondrial; nd = not detectable; ns = no sample.

‡Mean ± range of two assays.

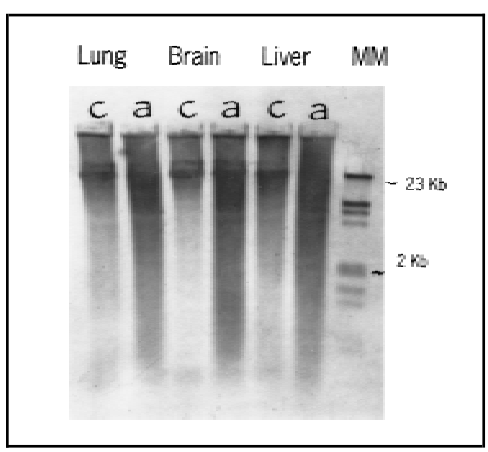

Fig. 2. Telomere length in nuclear DNA from lung, brain, and liver tissue of newborn mice either unexposed (c, control) or exposed (a) to 3′-azido-2′,3′-dideoxythymidine (AZT) *in utero* at a dose of 25.0 mg/day on days 12 through 18 of gestation. DNA was isolated, digested with restriction endonucleases, resolved in a 1% agarose gel, transferred to a nylon support membrane, and hybridized with a biotinylated probe specific for human telomeric DNA repeat sequences. The sizes of the telomeric repeats were determined by comparison with the biotinylated molecular marker (MM) DNAs (note the 2- and 23-kilobase reference regions). *See* ''Materials and Methods'' section for more details.

Again, there was a large interanimal variability in AZT-DNA levels among the monkey fetuses and in the DNA compartments. The size of telomeric DNA was not measurably altered in the DNA from liver, brain, cerebellum, heart, lungs, and placenta obtained from AZT-exposed fetal monkeys (data not shown).

Discussion

At the doses tested here, AZT is unequivocally a transplacental genotoxin and carcinogen in CD-1 mice. The liver and lungs, targets for tumor formation in this study, are typical organ sites for genotoxic transplacental carcinogens in mice *(7)*. The incidence, latency, multiplicity, and histopathology of the AZT-induced tumors indicate that AZT is intermediate in potency as a mouse transplacental carcinogen. On a toxic-equivalent dose basis, this drug is less potent than *N*-nitrosoethylurea *(29)*, 7,12-dimethylbenz[*a*]anthracene *(30)*, and 3-methylcholanthrene *(31)*, but it is more potent than *N*-nitrosodimethylamine *(29)* and the tobacco-specific nitrosamine 4-(methylnitrosamino)-1-(3-pyridyl)-1-butanone *(32)*. When given transplacentally to mice, benzo[*a*]pyrene produced lung and liver tumor multiplicities similar to those observed here *(30)*. The female reproductive organ tumors, absent in untreated animals, are similar in type and incidence to those resulting from mouse transplacental exposure to DES *(3)*.

In these experiments, AZT was given to mice for the last 37% of gestation at a daily dose that was approximately five-fold higher than the equivalent daily dose received by pregnant women [with the use of the mouse–human scaling factor of 1:12 described by Freireich et al. *(33)*]. With no scaling factors applied, an HIV-1-positive pregnant woman receiving AZT during the last two trimesters will have a total dose of about 1.4 g/kg body weight. The mice receiving 25.0 mg AZT/day were given a total dose of about 3.5 g/kg body weight, and the monkeys in this study received about 0.08 g AZT/kg body weight. Nevertheless, fetal *Erythrocebus patas* monkeys, given AZT at a much lower daily dose than that received by the CD-1 mice, had more AZT-DNA incorporation than that detected in the newborn mice.

Human–mouse dose comparisons are further complicated by a number of factors. Phosphorylation of AZT is more efficient in mice than in humans *(34)*. The plasma half-life of AZT in mice is 20 minutes *(35,36)*, whereas it is 1–2 hours in humans *(10)*. Because CD-1 mice typically carry 10–14 pups, the ratio of fetal weight to total maternal weight at deliv-

ery is 0.4 or more in the mouse, compared with 0.1 or less in humans. Together with tissue-specific differences in target organ responses and differences in litter size (11–14 pups for these experiments), the variability in AZT-DNA incorporation and telomere length might be expected. However, despite this variability, litter differences in tumorigenesis were not significant (Fig. 1). Pregnant monkeys, which carry only one fetus, may therefore be a more appropriate model for the human.

Two transplacental studies of AZT in mice, in which much lower doses than our doses of 12.5 and 25.0 mg/day were used, failed to find a carcinogenic effect. Ayers et al. *(37)* gave pregnant CD-1 mice 20.0 and 40.0 mg AZT/kg body weight per day (approximately 0.5 and 1.0 mg AZT/day) from the 10th day of gestation through weaning. Pups were then treated with 0, 20.0, or 40.0 mg AZT/kg body weight per day for 24 months. In animals given lifetime exposure to 40.0 mg/kg body weight per day, the males were unaffected, and vaginal tumors were observed only in the adult females; however, the tumor yield was not increased in animals given no drug exposure past weaning. Bilello et al. *(35)* gave 4.5 mg AZT/day to pregnant mice on days 16 through 21 of gestation and postnatally to nursing dams; these investigators did not detect tumors in the offspring by gross examination of tissues at 18 months. Taken together with our study, the data suggest that cumulative dose effects are critically important in determining the prenatal carcinogenicity of AZT.

Two novel genotoxicity assays were employed in this study. The AZT-RIA, which has previously been validated by comparison with incorporation of radiolabeled AZT into nuclear DNA *(22)*, was applied here for the first time to mitochondrial DNA. Unlike the situation with many chemical carcinogens that preferentially modify mitochondrial DNA by covalent binding, the incorporation of AZT into mitochondrial DNA was highly variable and did not parallel the incorporation of the drug into nuclear DNA. Because there is no literature for the comparison of nuclear and mitochondrial DNA incorporation of AZT, further validation must await confirmation and the development of alternative methods. Although it is unclear whether mitochondrial genotoxicity is related to tumorigenicity, it may be significant that mice developed tumors in organs where nuclear AZT DNA was not always detectable. In addition, the monkeys had higher levels of AZT incorporation into DNA than the mice in spite of receiving a much lower dose. The telomere length assays also provide novel information but no clear context for evaluation of the biologic consequences. The observation that telomeres were shortened in the mice and not in the monkeys would suggest that dose effects are important; however, the fetal mice appeared to function normally, and any possible relationship with the process of tumorigenesis remains obscure. Both of these biomarkers will be examined in great detail in future studies to assess their relationships with the observable biologic consequences of AZT exposure.

The relevance of the mouse studies to human exposure must be considered in the context of dose-equivalency, an especially difficult extrapolation for transplacental exposures. Available literature does not allow an accurate estimation of human risk implied by these data. However, our results suggest that the current practice of treating HIV-1-positive women and their infants with high doses of AZT could increase cancer risk in the drug-exposed children when they reach young adulthood or middle age. The remarkable effectiveness of AZT in preventing fetal HIV infection *(8,9)* indicates that the immediate need for treatment of a potentially fatal disease should outweigh the potential cancer risk. However, given the relatively high tumor incidences observed here at only half of the lifetime of the mouse, it would seem appropriate both to include additional notification in informed consent documents and to plan extensive follow-up of AZT-exposed children. In addition, since human carcinogenesis is multifactorial and takes many years to develop *(38)*, protective modulation may be possible *(39)*.

References

(1) Napalkov MP, Rice JM, Tomatis L, Yamasaki H, editors. Perinatal and multigeneration carcinogenesis. Lyon, France: IARC, 1989.

(2) Herbst AL, Ulfelder H, Poskanzer DC. Adenocarcinoma of the vagina. Association of maternal stilbestrol therapy with tumor appearance in young women. N Engl J Med 1971;284: 878–81.

(3) Newbold R. Cellular and molecular effects of developmental exposure to diethylstilbestrol: implications for other environmental estrogens. Environ Health Perspect 1995;103 Suppl 7: 83–7.

(4) Zahm SH, Devesa SS. Childhood cancer: overview of incidence trends and environmental carcinogens. Environ Health Perspect 1995; 103 Suppl 6:177–84.

(5) Savitz DA, Chen JH. Parental occupation and childhood cancer: review of epidemiologic studies. Environ Health Perspect 1990;88: 325–37.

(6) Bunin GR, Rose PG, Noller KL, Smith E. Occupational and environmental reproductive hazards. In: Paul M, editor. A guide for clinicians. Baltimore (MD): Williams & Wilkins, 1993:76–88.

(7) Anderson LM, Donovan PJ, Rice JM. Risk assessment for transplacental carcinogenesis. In: Li AP, editor. New approaches in toxicity testing and their application in human risk assessment. New York: Raven Press, 1985: 179–202.

(8) Connor EM, Sperling RS, Gelber R, Kiselev P, Scott G, O'Sullivan MJ, et al. Reduction of maternal–infant transmission of human immunodeficiency virus type 1 with zidovudine treatment. Pediatric AIDS Clinical Trials Group Protocol 076 Study Group. N Engl J Med 1994;331:1173–80.

(9) Sperling RS, Shapiro DE, Coombs RW, Todd JA, Herman SA, McSherry GD, et al. Maternal viral load, zidovudine treatment, and the risk of transmission of human immunodeficiency virus type 1 from mother to infant. Pediatric AIDS Clinical Trials Group Protocol 076 Study Group. N Engl J Med 1996;335: 1621–9.

(10) Retrovir. In: Physicians' desk reference. Montvale (NJ): Medical Economics Co., 1997: 1216–25.

(11) Ayers KM, Clive D, Tucker WE Jr, Hajian G, De Miranda P. Nonclinical toxicology studies with zidovudine: genetic toxicity tests and carcinogenicity bioassays in mice and rats. Fundam Appl Toxicol 1996;32:148–58.

(12) Toxicology and carcinogenesis studies of AZT. Research Triange Park (NC): National Toxicology Program, 1996.

(13) Olivero OA, Beland FA, Fullerton NF, Poirier MC. Vaginal epithelial DNA damage and expression of preneoplastic markers in mice during chronic dosing with tumorigenic levels of 3′-azido-2′,3′-dideoxythymidine. Cancer Res 1994;54:6235–42.

(14) Armitage P. Statistical methods in medical research. Oxford, England: Blackwell Scientific Publications, 1971:362–7.

(15) Colquhoun D. Lectures on biostatistics. Oxford, England: Clarendon Press, 1971: 116–23.

(16) Snedecor GW, Cochran WG. Statistical methods, sixth edition. Ames (IA): Iowa State University Press, 1967:215–21.

(17) Tarone RE. Testing the goodness of fit of the binomial distribution. Biometrika 1979;66: 585–90.

(18) Freeman MF, Tukey JW. Transformations related to the angular and the square root. Ann Math Statist 1950;21:607–11.

(19) Hollander M, Wolfe DA. Nonparametric statistical methods. New York: John Wiley and Sons, 1973:120–3.
(20) Hollander M, Wolfe DA. Nonparametric statistical methods. New York: John Wiley and Sons, 1973:67–74.
(21) Tamura K, Aotsuka T. Rapid isolation method of animal mitochondrial DNA by the alkaline lysis procedure. Biochem Genet 1988;26: 815–9.
(22) Olivero OA, Beland FA, Poirier MC. Immunofluorescent localization and quantitation of 3′-azido-2′,3′-dideoxythymidine (AZT) incorporated into chromosomal DNA of human, hamster and mouse cell lines. Int J Oncol 1994; 4:49–54.
(23) Lu LJ, Anderson LM, Jones AB, Moskal TJ, Salazar JJ, Hokanson JA, et al. Persistence, gestation stage-dependent formation and interrelationship of benzo[*a*]pyrene-induced DNA adducts in mothers, placentae and fetuses of *Erythrocebus patas* monkeys. Carcinogenesis 1993;14:1805–13.
(24) Gomez DE, Kassim A, Olivero OA. Preferential incorporation of 3′-azido-2′,3′-dideoxythymidine (AZT) in telomeric sequences of CHO cells. Int J Oncol 1995;7:1057–60.
(25) Maniatis TE, Fritsch EF, Sambrook J. Molecular cloning: a laboratory manual. Cold Spring Harbor (NY): Cold Spring Harbor Laboratory Press, 1982.
(26) Percy DH, Jonas AM. Incidence of spontaneous tumors in CD (R) -1 HaM-ICR mice. J Natl Cancer Inst 1971;46:1045–65.
(27) Kim NW, Piatyszek MA, Prowse KR, Harley CB, West MD, Ho PL, et al. Specific association of human telomerase activity with immortal cells and cancer. Science 1994;266:2011–5.
(28) Gomez DE, Olivero OA. Long-term AZT (3′-azido-2′,3′-dideoxythymidine) treatment shortens the telomeric sequences of HeLa cells in culture [abstract]. Proc Am Assoc Cancer Res 1996;36:abstract 3848.
(29) Anderson LM, Hagiwara A, Kovatch RM, Rehm S, Rice JM. Transplacental initiation of liver, lung, neurogenic, and connective tissue tumors by *N*-nitroso compounds in mice. Fundam Appl Toxicol 1989;12:604–20.
(30) Anderson LM, Ruskie S, Carter J, Pittinger S, Kovatch RM, Riggs CW. Fetal mouse susceptibility to transplacental carcinogenesis: differential influence of Ah receptor phenotype on effects of 3-methylcholanthrene, 7,12-dimethylbenz[*a*]anthracene, and benzo[*a*]pyrene. Pharmacogenetics 1995;5:364–72.
(31) Anderson LM, Jones AB, Riggs CW, Ohshima M. Fetal mouse susceptibility to transplacental lung and liver carcinogenesis by 3-methylcholanthrene: positive correlation with responsiveness to inducers of aromatic hydrocarbon metabolism. Carcinogenesis 1985;6:1389–93.
(32) Anderson LM, Hecht SS, Dixon DE, Dove LF, Kovatch RM, Amin S, et al. Evaluation of the transplacental tumorigenicity of the tobacco-specific carcinogen 4-(methylnitrosamino)-1-(3-pyridyl)-1-butanone in mice. Cancer Res 1989;49:3770–5.
(33) Freireich EJ, Gehan EA, Rall DP, Schmidt LH, Skipper HE. Quantitative comparison of toxicity of anticancer agents in mouse, rat, hamster, dog, monkey and man. Cancer Chemother Rep 1966;50:219–44.
(34) Balzarini J, Pauwels R, Baba M, Herdewijn P, De Clercq E, Broder S, et al. The *in vitro* and *in vivo* anti-retrovirus activity, and intracellular metabolism of 3′-azido-2′,3′-dideoxythymidine and 2′,3′-dideoxycytidine are highly dependent on the cell species. Biochem Pharmacol 1988;37:897–903.
(35) Bilello JA, MacAuley C, Fredrickson TN, Bell MM, McKissick C, Shapiro SG, et al. Use of a neonatal murine retrovirus model to evaluate the long-term efficacy and toxicity of antiviral agents. Ann N Y Acad Sci 1990;616: 238–51.
(36) Bilello JA, Eiseman JL, Standiford HC, Drusano GL. Impact of dosing schedule upon suppression of a retrovirus in a murine model of AIDS encephalopathy. Antimicrob Agents Chemother 1994;38:628–31.
(37) Ayers KM, Torrey CE, Reynolds DJ. A transplacental carcinogenicity bioassay in CD-1 mice with Zidovudine. Fundam Appl Toxicol 1997;38:195–8.
(38) Yuspa SH, Poirier MC. Chemical carcinogenesis: from animal models to molecular models in one decade. Adv Cancer Res 1988;50: 25–70.
(39) Greenwald P, Malone WF, Cerny ME, Stern HR. Cancer prevention research trials. Adv Cancer Res 1993;61:1–23.

Notes

We extend our appreciation to Drs. Jerrold Ward and Miriam Anver for review of the pathology slides and to Dr. Robert Tarone for verifying the statistics. For review of the data and the manuscript, we thank Drs. Richard D. Klausner, George Vande Woude, Alan S. Rabson, Henry C. Pitot, Lorenzo Tomatis, and Paul Kleihues. For editorial assistance, we thank Ms. Margaret Taylor.

Manuscript received March 7, 1997; revised August 20, 1997; accepted August 28, 1997.

High Telomerase Activity in Primary Lung Cancers: Association With Increased Cell Proliferation Rates and Advanced Pathologic Stage

Juan Albanell, Fulvio Lonardo, Valerie Rusch, Monika Engelhardt, John Langenfeld, Wei Han, David Klimstra, Ennapadam Venkatraman, Malcolm A. S. Moore, Ethan Dmitrovsky[*]

Background: **Telomerase enzyme activity is not detected in most normal cells, a phenomenon believed to be associated with limitations on cellular proliferation. Since this activity is detected in nearly all human tumors, including non-small-cell lung cancers, it has been suggested that telomerase activation may be coupled to acquisition of the malignant phenotype. In this study, we determined whether telomerase activity was associated with tumor pathologic stage, tumor cell proliferation rates, and clinical outcome in a cohort of patients with resected non-small-cell lung cancer for whom long-term follow-up was available.** ***Methods:*** **Primary tumor specimens from 99 patients treated with surgery alone and six patients treated with surgery after chemotherapy were analyzed. Telomerase activity was measured by means of a modified Telomeric Repeat Amplification Protocol (TRAP) assay. Southern blot analysis of terminal restriction fragments was used to evaluate telomere length. Immunohistochemical analysis of Ki-67, a proliferation-associated nuclear antigen, was used to assess tumor cell proliferation.** ***Results:*** **Telomerase activity was detected in 84 of the 99 tumors treated with surgery alone; this activity was not detected in specimens of adjacent, benign lung tissue. Telomerase was detected in only three of six tumors resected after chemotherapy. For the surgery-alone group, statistically significant positive associations were found between the level of telomerase activity and tumor stage, lymph node metastasis, pathologic TNM (tumor–node–metastasis) stage, and Ki-67 immunostaining; a statistically significant inverse association was found between telomerase activity and patient age. No statistically significant differences in telomere length were found in relation to telomerase activity or pathologic stage. Telomerase activity was not found to be associated with clinical outcome in a multivariate Cox proportional hazards analysis adjusted for tumor stage and lymph node status.** ***Conclusions:*** **High telomerase activity is detected frequently in primary non-small-cell lung cancers that exhibit high tumor cell proliferation rates and advanced pathologic stage. [J Natl Cancer Inst 1997;89:1609–15]**

Human telomeres are specialized nucleoprotein structures located at the ends of chromosomes and are composed of tandem repeats of the sequence 5′-TTAGGG-3′ bound to specific proteins. Conventional DNA polymerases cannot replicate the ends of linear chromosomes, resulting in gradual telomere shortening when cells divide *(1).* Telomerase is a ribonucleoprotein that synthesizes *de novo* telomeric DNA onto chromosome ends, thus compensating for this ''end-replication problem'' *(2,3).* In somatic cells, where telomerase activity is usually not detected, there is progressive telomere shortening during replication, and telomere length often reflects cellular proliferative potential *(4–7).* In contrast, germ cells and most immortalized human cell lines exhibit telomerase activity and stable telomere length *(8–10).* Telomerase activity is frequently expressed in human tumors, as assessed by the highly sensitive polymerase chain reaction (PCR)-based Telomeric Repeat Amplification Protocol (TRAP) assay *(8).* These findings, coupled with infrequent telomerase expression in normal cells, suggested that telomerase activation was tightly coupled to the acquisition of the malignant phenotype *(8,11,12).*

The RNA component of human telomerase *(13)* and a telomerase-associated protein have recently been cloned *(14).* These two components are widely expressed in human tumors and tumor cell lines, and they may be necessary for telomere elongation *(13,14).* In support of this possibility, treatment of immortalized human tumor cell lines with antisense oligodeoxyribonucleotides targeted to the RNA component of human telomerase led to a reinitiation of telomere shortening and induction of the massive cell death associated with proliferative senescence *(13).* The maintenance of a constant average telomere length in cells expressing telomerase activity seems to be regulated by a negative feedback loop. This idea is supported by functional studies with a recently cloned telomere-binding protein that suppresses telomere elongation and is proposed to be a negative regulator of telomerase activity *(15).*

Lung cancer remains the most common cause of cancer-related death in the United States for both men and women. A better understanding of the biology of lung tumors and identification of diagnostic markers or new therapeutic targets are urgently needed to develop novel treatment strategies that could improve the dismal survival rates of most patients with lung cancer *(16,17).* In a pivotal study *(18),* telomerase activity was found in 78.4% of non-small-cell lung cancers (NSCLCs) and in all small-cell lung cancers examined. Varying levels of telomerase activity were previously detected in NSCLCs *(18),* and it was hypothesized that the tumors with no or low telomerase activity might be composed primarily of mortal cancer cells. High levels of telomerase activity were detected in metastatic lesions even when undetected in the primary tumor, suggesting that telomerase activation contributes to the development

**Affiliations of authors:* J. Albanell, M. Engelhardt, W. Han, M. A. S. Moore (Laboratory of Developmental Hematopoiesis), F. Lonardo (Department of Pathology and Laboratory of Molecular Medicine), V. Rusch, J. Langenfeld (Thoracic Surgery Service, Department of Surgery, and Laboratory of Molecular Medicine), D. Klimstra (Department of Pathology), E. Venkatraman (Biostatistics Service, Department of Epidemiology and Biostatistics), E. Dmitrovsky (Division of Solid Tumor Oncology, Department of Medicine, and Laboratory of Molecular Medicine), Memorial Hospital and Sloan-Kettering Institute, Memorial Sloan-Kettering Cancer Center, New York, NY.

Correspondence to: Ethan Dmitrovsky, M.D., Memorial Sloan-Kettering Cancer Center, 1275 York Ave., New York, NY 10021.

See ''Notes'' following ''References.''

of metastatic disease. This study *(18)* raised the prospect that telomerase might represent a marker for immortal lung cancer cells and a therapeutic target in lung cancer.

In our study, telomerase activity was measured by use of a recently modified TRAP assay (Kim NW, Wu F: personal communication) that increases the reliability of the assay, allows the expression of relative levels of telomerase activity, and identifies the presence of inhibitors of *Taq* polymerase. The purpose of this study was to analyze comprehensively whether a relationship existed between telomerase activity, tumor pathologic stage, tumor cell proliferation rates, and clinical outcome in a well-characterized cohort of patients with resected NSCLC for whom long-term clinical follow-up was available.

Methods

Tissue specimens. One hundred seven tissue specimens were obtained from consecutive patients with primary NSCLC who underwent potentially curative operations. Use of these found tissue specimens was approved by the relevant institutional review boards. Protein extracts from 105 of these specimens were adequate for analysis. Pulmonary resection was accompanied by careful intraoperative staging with complete mediastinal lymph node dissection as described by Martini and Flehinger *(19)*. Lymph nodes were labeled separately for pathologic analysis, in conformity with the American Thoracic Society Lymph Node Map *(20)*. Within 10 minutes of completion of the pulmonary resection, a sample of the primary tumor, trimmed of the surrounding lung tissue and of any grossly necrotic material, was snap frozen in liquid nitrogen. A separate specimen of benign lung tissue was harvested from an area distant from the primary tumor and also frozen in liquid nitrogen. The presence of malignant or benign lung tissue in the harvested samples was confirmed by microscopic examination. An independent assessment by two pathologists (F. Lonardo and D. Klimstra) was performed, and both pathologists concurred with respect to the histopathologic features evaluated. The specimens were scored for tumor grade, proportion of tumor tissue present, proportion of necrosis in the tumors, and the estimated percentage of infiltrating lymphocytic cells in areas with tumor. The tumor–node–metastasis (TNM) stage was determined according to the International Staging System for NSCLC *(21)*.

Protein extraction. Frozen tissue samples (50–100 mg) were homogenized in 100–200 μL ice-cold CHAPS (3-[{3-cholamidopropyl}-dimethylammonio]-1-propane-sulfonate) lysis buffer (0.5% CHAPS, 10 m*M* Tris–HCl [pH 7.5], 1 m*M* $MgCl_2$, 1 m*M* EGTA, 10% glycerol, 5 m*M* β-mercaptoethanol, and 10 ng/mL leupeptine) with the use of disposable pestles and standard techniques. The tissue homogenates were incubated on ice for 30 minutes and then centrifuged at 12 000*g* for 30 minutes at 4 °C. Supernatants were collected and stored at −80 °C. Protein concentrations were measured by use of the Bio-Rad protein assay kit (Bio-Rad Laboratories, Richmond, CA), and aliquots containing 1 μg protein/mL were stored at −80 °C *(8,22,23)*.

TRAP assay. The telomerase assay was performed according to a recently modified TRAP assay protocol (Kim NW, Wu F: personal communication) *(8,22–24)*. Extracts containing 2 μg of protein were assayed in reaction tubes that contained 50 μL of the TRAP reaction mixture. The TS primer was labeled at its 5′ end by use of 5 U T4 polynucleotide kinase (PNK; Promega Corp., Madison,WI) and 2.5 μCi of 3000 Ci/mmol [γ-^{32}P]adenosine triphosphate per 1 μg of TS. The kinase reaction mixture was incubated at 37 °C for 20 minutes, and then the PNK was heat inactivated at 95 °C for 5 minutes. Each TRAP reaction consisted of 5 μL 10× TRAP buffer *(22)*, 50 μ*M* standard deoxyribonucleoside triphosphates, 0.1 μg end-labeled TS primer, 0.1 μg RP return primer, 0.1 μg NT internal control primer, 0.01 amol of the TSNT internal control template, 2 U *Taq* DNA polymerase (AmpliTaq; The Perkin-Elmer Corp., Branchburg, NJ), and the extract containing 2 μg protein. TSNT is an internal control PCR template amplified by the primers TS and NT, giving a 36-base-pair (bp) product. After a 30-minute incubation at room temperature, the TRAP reaction mixture was subjected to 30 cycles of PCR. The PCR products were resolved by electrophoresis in a 15% polyacrylamide gel under nondenaturing conditions, and the gel was analyzed on a Phosphorimager (Molecular Dynamics, Sunnyvale, CA). In every gel, the products of a negative control reaction (2 μL CHAPS lysis buffer) and of 0.1 amol of the quantitation standard oligonucleotide R8 were included. The telomerase quantitation results were expressed as total product generated (TPG) (*see* Fig. 1 for details of the quantitation). The specificity of the 6-bp ladders was confirmed by the absence of the ladders following heat inactivation of the protein extracts. All protein extracts were analyzed in at least two independent TRAP assays, and the average telomerase activity (TPG) was calculated (Fig. 1). Subgroups were defined as having negative (TPG = 0), low (TPG>0 and ⩽5), moderate (TPG>5 and ⩽30), or high (TPG>30) telomerase activity.

Alkaline phosphatase activity. Alkaline phosphatase activity was assayed as a control for possible protein degradation *(23)*. Two tumor protein extracts had no detectable alkaline phosphatase activity and were not subsequently analyzed. Alkaline phosphatase levels were similar in extracts of normal and malignant tissues (data not shown).

Immunohistochemistry. Ki-67, a proliferation-associated nuclear antigen that is present only in proliferating cells *(25)*, was assessed immunohistochemically to measure tumor cell proliferation rates. Five-micron-thick, paraffin-embedded sections were deparaffinized and rehydrated by use of standard techniques. Pretreatment of the sections consisted of digestion with 0.05% trypsin, followed by microwave treatment for 10 minutes. The sections were then exposed to 3% H_2O_2 for 5 minutes, saturated with 0.05% bovine serum albumin (BSA), and preincubated with normal horse serum (Cappel Research, Durham, NC) at a 1:20 dilution in 2% BSA–

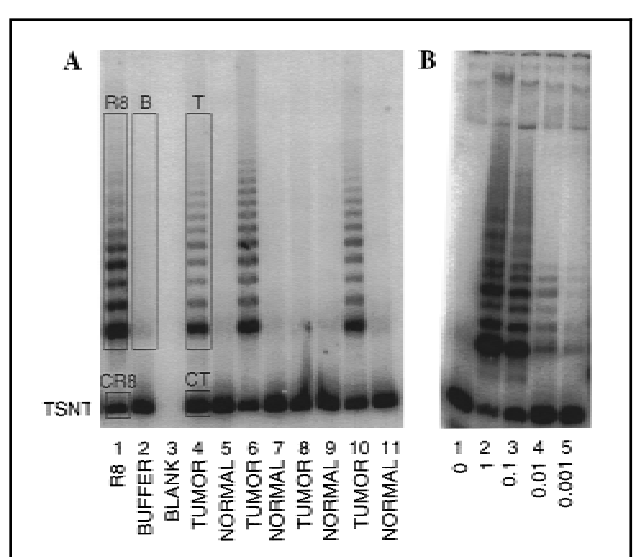

Fig. 1. Telomerase activity was measured by use of a recently modified Telomeric Repeat Amplification Protocol (TRAP) assay (*see* text for details). **Panel A** displays the R8 quantitation standard (lane 1), negative control results (Buffer [no extract], lane 2), and the TRAP products generated from extracts of selected pairs of non-small-cell lung carcinoma and histologically benign lung tissue (lanes 4–11). The R8 quantitation standard oligonucleotide exhibits a characteristic pattern of six bands corresponding to the first through sixth TRAP products. The assay incorporates an internal polymerase chain reaction (PCR) control, yielding a 36-base-pair (bp) product (designated TSNT), which migrates in the analytic polyacrylamide gel at a position 14 bp below the smallest TRAP band. This control is used to monitor PCR efficiency during the PCR step of the assay. The amount of telomerase activity from a given reaction was calculated by use of the following formula: TPG = $[(T - B)/(CT)]/[(R8 - B)/(CR8)] \times 100$, where T = the radioactive counts from the telomerase bands from the protein extract, B = the counts from the negative control reaction (background), $R8$ = the counts from the R8 standard (0.1 amol), CT = the counts from the internal control TSNT reaction (0.01 amol) of the protein extract, and $CR8$ = the counts from the TSNT reaction (0.01 amol) of the R8 standard (0.1 amol). The final quantitation was expressed as the TPG (total product generated). One unit of TPG was defined as 0.001 amol (or 600 molecules) of TS primer extended by at least three telomeric repeats by the telomerase present in the extract. A telomerase activity level of 1 TPG corresponds approximately to the telomerase activity from one immortal cell (Kim NW, Wu F: personal communication). **Panel B** shows that the assay was in the linear range from 0.001 amol (1 TPG) to 1 amol (1000 TPG) of R8 standard. This range extended over three logarithms (base 10) of the target protein concentrations.

phosphate-buffered saline (PBS) for 15 minutes at room temperature. The MIB-1 antibody (Immunotech, Westbrook, ME), used at a 1:50 dilution in 2% BSA–PBS, was applied at 4 °C for 16 hours *(25)*. The sections were then rinsed with PBS for 30 minutes, and a biotinylated anti-mouse immunoglobulin G (Vector Laboratories, Inc., Burlingame, CA) was applied at a 1:500 dilution in 1% PBS–BSA at room temperature for 60 minutes. The sections were rinsed with PBS and incubated with peroxidase-conjugated streptavidin (Dako Corp., Carpinteria, CA) at a 1:500 dilution in 1% BSA–PBS at room temperature for 45 minutes. The sections were then rinsed with PBS for 30 minutes, and color from the chromogen diaminobenzidine (0.06% in PBS) was developed for 15 minutes. The sections were subsequently rinsed in water, counterstained with Harris-modified hematoxylin (Fisher Scientific Co., Pittsburgh, PA), rinsed in 1% acid alcohol for 2 seconds, rinsed in ammonia water for 15 seconds, dehydrated, and placed under coverslips in permount media. Ki-67 immunostaining was scored as the percentage of positive tumor cells per section.

Terminal restriction fragment (TRF) length measurements. For DNA isolation, tissues were incubated for at least 3 hours at 50 °C with an appropriate volume of DNA extraction buffer (100 m*M* NaCl, 40 m*M* Tris [pH 8.0], 20 m*M* EDTA [pH 8.0], 0.5% sodium dodecyl sulfate, and 0.1 mg/mL proteinase K), followed by phenol–chloroform–isoamyl alcohol extractions and precipitation with 3 *M* sodium acetate and ethanol. Electrophoresis of the undigested, high-molecular-weight DNA was performed to assess DNA degradation. Southern blot analysis to estimate telomere length was based on previously reported methods *(4–7,26)*. Genomic DNA was digested with *Msp* I and *Rsa* I restriction endonucleases (Boehringer Mannheim, Mannheim, Germany) at 37 °C for an appropriate length of time. Completeness of the DNA digestion was confirmed by means of gel electrophoresis; 10 μg of digested DNA was subjected to electrophoresis in 0.5% agarose gels. The resolved DNA was depurinated for 20 minutes in 0.2 *M* HCl, denatured for 30 minutes in 0.5 *M* NaOH–1.5 *M* NaCl, and neutralized for 30 minutes in 0.5 *M* Tris (pH 8.0)–1.5 *M* NaCl. The DNA was then blotted overnight onto nylon filters (Schleicher and Schuell, Inc., Keene, NH) in 20× solution of sodium chloride and sodium citrate (SSC). The filters were dried at 80 °C for 1 hour and subsequently hybridized to a $^{32}PO_4$ end-labeled $(TTAGGG)_3$ probe (Genset, La Jolla, CA) in a mixture that contained 5× SSC, 5× Denhardt's solution, 10 m*M* phosphate buffer (pH 6.4), and 30 μg/mL salmon sperm DNA at 50 °C overnight. The filters were washed twice in 0.5× SSC–0.1% sodium dodecyl sulfate for 15 minutes each at 50 °C and then at room temperature for an appropriate length of time. To determine TRF length, the hybridized probe was visualized with a Phosphorimager (Molecular Dynamics), which quantified the radioactive signal in each of the lanes. Each lane was then graphically divided over the range of 2–23 kilobase pairs (kbp) into quadrants, and the densitometric counts in each quadrant were measured. The molecular-weight range of each quadrant was determined by use of radioactive markers. The mean and peak TRF lengths were calculated as described *(26)*.

Clinical database. After pulmonary resection, the patients were seen in follow-up by one surgeon (V. Rusch), as previously reported *(16)*. The parameters that were recorded included the patient's age and sex, the tumor histology and stage, the estimated percentage of viable tumor cells present in the specimen, and the disease-free and overall survivals as calculated from the date of surgery. The telomerase activity, TRF length, and Ki-67 immunostaining results were evaluated without knowledge of the clinical outcomes.

Statistical analysis. Associations between telomerase activity (TPG) and the sex of the patient, tumor histology, lymph node metastasis, T stage, N stage, and pathologic TNM stage were evaluated by use of the Kruskal–Wallis test *(27)*. Spearman's rank correlations *(27)* were determined between telomerase activity and patient age, Ki-67 immunostaining, percentage of tumor cells in the specimen, percentage of necrosis in the specimen, and percentage of lymphocytic infiltration. The distribution of telomerase activity in relation to the degree of tumor cell differentiation was compared by use of the Wilcoxon test *(27)*. Overall survival and disease-free survival were calculated from the date of thoracotomy by use of the method of Kaplan and Meier *(28)*. The log-rank test *(29)* was used to compare survival across the subgroups of telomerase activity. All statistical tests were conducted at the two-sided, .05 level of significance. Proportional hazards regression was used to test the prognostic significance of factors in a multivariate model *(30)*.

Results

Telomerase Activity and Histopathology

A total of 105 NSCLC specimens from 105 patients were examined in this study. Histologically benign lung tissue adjacent to 34 of these NSCLC specimens was also examined. Ninety-eight patients with stage I-IIIA tumors and one patient with stage IV disease were treated by surgical resection alone (Table 1); six patients had preoperative chemotherapy. The patients were treated during the period from January 1990 through May 1996, and clinical follow-up was updated as of September 1996. Telomerase activity was present in 84 (84.8%) of the 99 tumors from patients treated with surgical resection alone. Among these 84 tumors, 31 had low, 32 had moderate, and 21 had high telomerase activity (Fig. 1; data not shown). The linearity of the TRAP assay was confirmed over a three-logarithm (base 10) range of the target protein concentrations (Fig. 1, B). The average level of telomerase activity was 20 TPG (range, 0–134.9) (Fig. 2, A). Telomerase activity was not detected in 15 (15.2%) of the 99 tumors in addition to all adjacent, histologically benign lung tissue specimens examined (Fig. 1, A; data not shown). A histopathologic review of 81 of the tumors established that telomerase activity and the estimated percentage of tumor cells present in the specimen ($P = .1$), the proportion of necrosis in the specimen ($P = .72$), the degree of lymphocytic infiltration ($P = .1$), or the histologic grade of the tumor ($P =$

Table 1. Comparison of tumor histology, primary tumor size, lymph node metastasis, and tumor stage with telomerase activity in primary, resected non-small-cell lung cancer*

		Telomerase activity		
	No. of tumors	Negative	Positive	% positive
Histology				
Adenocarcinoma	56	8	48	85.7
Squamous cell carcinoma	36	6	30	83.3
Large-cell carcinoma	7	1	6	85.7
Tumor stage				
T1	20	1	19	95.0
T2	66	13	53	80.3
T3	13	1	12	92.3
Lymph node status				
N0	63	13	50	79.4
N1	20	1	19	95.0
N2	16	1	15	93.8
Pathologic stage				
I	55	12	43	78.2
II	18	1	17	94.4
IIIA	25	2	23	92.0
IV†	1	0	1	100.0
Total	99	15	84	84.8

**See (21)* for information on tumor staging.

†The corresponding patient had a simultaneous solitary brain metastasis that was resected prior to thoracotomy.

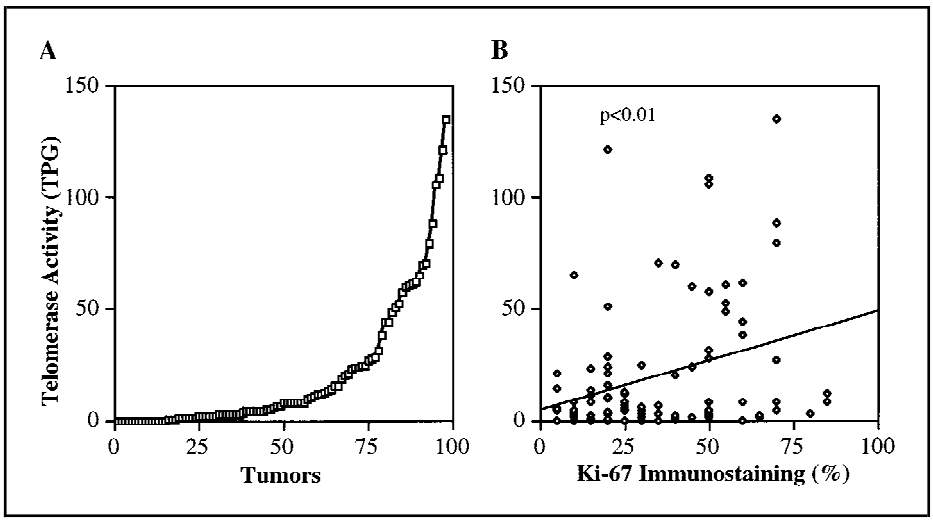

Fig. 2. A) Total product generated (TPG), as a measure of the level of telomerase activity in primary, non-small-cell lung cancers, shows the continuum of the activity detected. **B)** The proliferative cell fraction was assessed by means of immunohistochemistry, using the antibody MIB-1, which recognizes the Ki-67 proliferation-associated nuclear antigen in paraffin-embedded tissue specimens. The percentage of Ki-67 staining tumor cells was correlated with telomerase activity (TPG) (r = +.29; P<.01). *See* text for additional details.

.62) were not linked. Telomerase activity was not associated with the sex of the patient (P = .47) or the histologic tumor type (P = .87) (Table 1). Patient age was correlated inversely with telomerase activity (r = –.4; P<.01). The remaining six patients had stage IIIA tumors that were treated by surgical resection after induction chemotherapy; the data from these patients were analyzed separately.

Telomerase Activity and Tumor Cell Proliferation Rate

The MIB-1 antibody and immunostaining were used to measure the tumor cell proliferation rates in 93 tumors. The percentage of Ki-67-positive tumor cells correlated with telomerase activity (r = +.29; P<.01; Fig. 2, B). In telomerase-negative tumors, the average percentage of MIB-1 immunostaining tumor cells was 22%; for the telomerase-positive tumors, this percentage was 32%, 32%, and 49% for cases with low, moderate, and high telomerase activity, respectively.

Telomerase Activity and Pathologic Stage

Telomerase activity was detected in 95.0% of T1, 80.3% of T2, and 92.3% of T3 tumors (Table 1). The average telomerase activity (TPG) was 18 in T1 and T2 tumors compared with 36 in T3 tumors (P = .03) (Fig. 3, A, left panel). A significant association was found between telomerase activity and lymph node metastasis (N0 versus N1–2, P = .05; Fig. 3, A, middle panel). Telomerase activity was detected in 79.4% of N0, 95.0% of N1, and 93.8% of N2 tumors (Table 1). The average telomerase activity (TPG) was 18.3 in N0 lesions, 16.2 in N1 lesions, and 32.7 in N2 lesions. Telomerase activity was associated with tumor pathologic stage, with average telomerase activities (TPGs) of 14.8, 18.2, and 30.2 in stages I, II, and IIIA, respectively (P = .01 stage I versus stage II versus stage IIIA; P<.01 for stage I versus stages II–IIIA; Fig. 3, A, right panel). Telomerase activity was detected in 78.2% of stage I, 94.4% of stage II, and 92.0% of stage IIIA

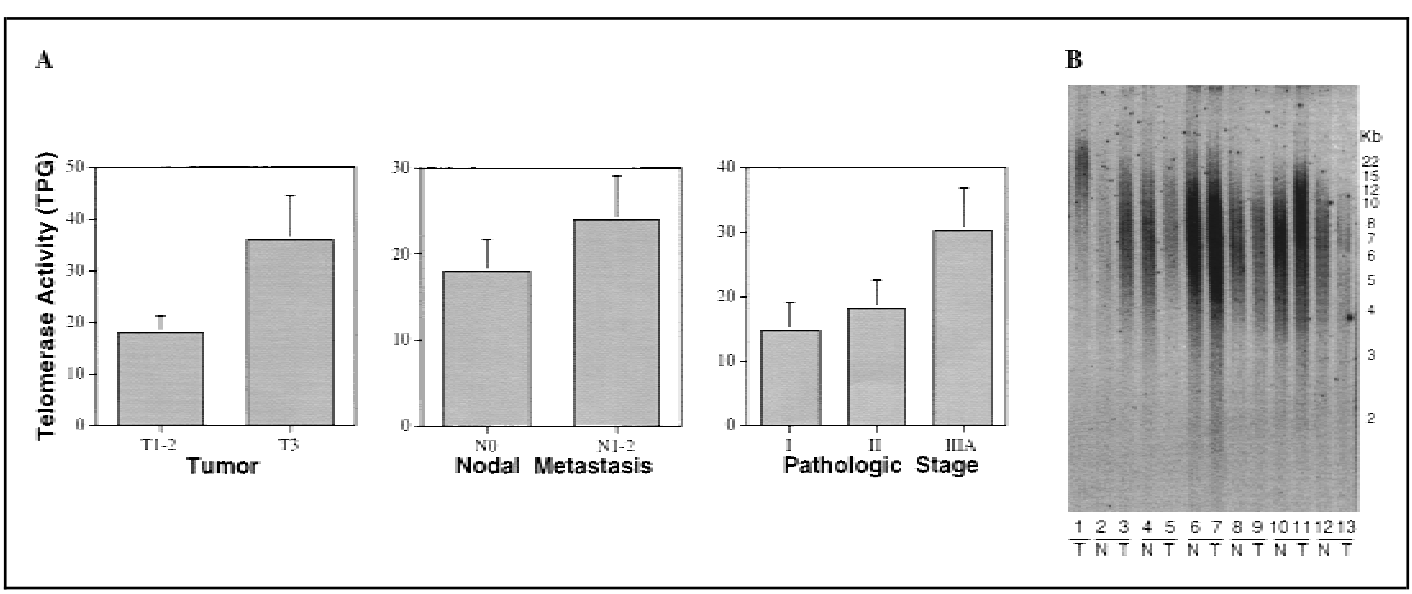

Fig. 3. A) Telomerase activity (average total product generated [TPG] ± standard error of the mean [SEM]) was associated with tumor size and extension of the primary lesion (left panel, two-sided P = .03), the presence of lymph node metastasis (middle panel, two-sided P = .05), and pathologic TNM stage *(21)* (right panel, two-sided P = .01) in non-small-cell lung cancer. **B)** The Southern blot analysis of terminal restriction fragments (TRFs) in lung tumors. The tumor in lane 1 showed a long TRF (approximately 23 kilobases [kb]) and had high telomerase activity; DNA from matched, benign lung tissue was unavailable for this specimen. TRFs from representative tumor (T) and matched, histologically benign (N) lung tissue specimens are shown in lanes 2–13. Tumor mean TRF lengths were found to be similar to mean TRF lengths in matched benign lung tissue (compare lanes 2, 6, and 8 with lanes 3, 7, and 9, respectively), longer than mean TRF lengths in matched benign lung tissue (compare lane 4 with lane 5 and lane 10 with lane 11), or shorter than mean TRF lengths in matched benign lung tissue (compare lane 12 with lane 13). The sizes of molecular weight standards appear at the right of this figure. *See* text for additional details.

tumors (Table 1). One patient with stage IV (simultaneous solitary brain metastasis that was resected prior to thoracotomy) had a TPG of 108.

Telomerase Activity and Telomere Length

The mean TRF length ranged from 6.2 to 10.4 kbp in the 15 telomerase-negative tumors and from 5.5 to 23.0 kbp in the 30 telomerase-positive tumors examined (Fig. 3, B; data not shown). In telomerase-positive tumors, average mean TRFs were 7.5 kpb, 8.2 kbp, and 8.2 kbp in specimens with low, moderate, and high telomerase activity, respectively. No significant association between TRF length and tumor size, lymph node metastasis, or pathologic stage was found. In 34 cases, TRF analysis was performed in both the tumor and adjacent, histologically benign lung tissue. Similar mean TRFs were measured in 26 (76%) cases, but TRFs were reduced in the tumor in six (18%) cases and elongated in the tumor in two (6%) cases. Peak TRF values were similar between the tumor and benign lung tissue in 23 (68%) cases but were reduced in the tumor in eight (24%) cases and elongated in the tumor in three (9%) cases. Among the four telomerase-negative tumors, the TRF lengths were similar to those found in normal tissues in three cases and reduced in the tumor in one case. The average telomerase activities (TPGs) were 16, 13, and 18 in tumors with elongated, reduced, and unchanged TRF lengths, respectively.

Telomerase Activity and Clinical Outcome

There were no statistically significant differences in disease-free survival or overall survival between patients grouped on the basis of telomerase activity ($P = .1$; data not shown). The 3-year actuarial disease-free survival was 57% for patients with telomerase-negative tumors compared with 40% for patients whose tumors had high telomerase activity, but this difference was not statistically significant.

The prognostic significance of telomerase activity was measured by use of a Cox proportional hazards model. Since T status and N status are known prognostic factors in lung cancer, these parameters were included in the analysis. The hazards ratios (and 95% confidence intervals) for overall survival were 1.78 (1.23–2.56) for $T \leq 2$ versus $T > 2$, 0.66 (0.48–0.91) for $N = 0$ versus $N > 0$, and 1.07 (0.63–1.82) for telomerase-negative versus -positive cases. Similarly, the hazard ratios (and 95% confidence intervals) for disease-free survival were 1.77 (1.25–2.52), 0.61 (0.45–0.82), and 1.24 (0.74–2.08), respectively. No statistically significant association was found between telomerase activity and clinical outcome after this analysis.

Telomerase Activity in Stage IIIA NSCLC After Preoperative Chemotherapy

Telomerase activity was not detected in three of six primary stage IIIA tumors resected after induction chemotherapy *(31)* (data not shown). The three telomerase-negative tumors had a major pathologic response to chemotherapy. The remaining three tumors had detectable telomerase activity and a less marked response to neoadjuvant chemotherapy.

Discussion

This study extends previous work *(18)* by demonstrating that high telomerase activity in primary NSCLC is frequent in specimens with high cellular proliferation rates and is associated with tumors presenting with advanced stage. Telomerase activity was detected in 84.8% of the NSCLC specimens from patients who underwent surgical resection only. Telomerase activity was significantly higher in advanced-stage disease than in early-stage disease. Telomerase activity was inversely associated with age, as has been seen with at least one other tumor *(32)*. Telomerase activity has been linked to tumor stage in previous studies of neuroblastoma *(33)*, breast cancer *(34)*, gastric cancer *(35)*, and leukemias *(36)*. However, such an association was not found in studies of renal cancer *(37)*, breast cancer *(32,38)*, gynecologic tumors *(39)*, or hepatocellular carcinoma *(40)*.

In this series, telomerase-negative tumors were infrequently associated with lymph node metastasis at presentation. This finding could relate to the need for extensive cell proliferation for metastasis to develop from individual clones. The clonal expansion required could lead to critically reduced telomere lengths in the absence of telomerase reactivation, limiting the potential for metastatic progression. In three of six stage IIIA NSCLC cases having major pathologic responses to chemotherapy, telomerase activity was not detected in the tumors after chemotherapy. Perhaps repressed telomerase activity results from effective chemotherapeutic treatment. Examining this possibility should be the subject of future work.

A modified PCR-based telomerase assay was used in this study. It is worth noting that some variables could have influenced the telomerase activity measurements. For instance, alkaline phosphatase measurements were used to assess the integrity of extracted protein. However, the stability of alkaline phosphatase activity may not parallel the stability of telomerase activity, which could be more sensitive to minor protein degradation in the extracts. The efficiency of protein extraction may also have varied between the analyzed tissue specimens. While the percentage of tumor cells present in adjacent tissues was scored, the percentage of tumor cells present in the specimens used for telomerase activity measurements was not scored, since the same tissue cannot be processed for both parameters.

A small proportion of human tumors does not exhibit telomerase activity *(41,42)*. In our study, telomerase activity was not detected in 15.2% of the primary lung cancers treated by surgical resection alone. In a study of retinoblastoma, a developmental tumor with a limited number of associated mutations, telomerase activity was absent in 50% of the examined tumors *(43)*. It is possible that the requirement for telomerase in tumorigenesis depends on the telomere lengths found in precursor cells and on the number of clonal expansions needed *(41)*. Additional explanations for telomerase-negative tumors include the following: 1) telomerase activation followed by its repression after telomere elongation, 2) telomerase down-regulation associated with cellular quiescence, 3) telomerase activity below the level of detection of available assays, or 4) alternative mechanisms to compensate for the end-replication problem. The existence of an alternative pathway was reported in immortalized cell lines and was associated with very long telomeres (up to 50 kbp) *(44)*. However, very long telomeres were not found in this study for the 15 telomerase-negative NSCLC speci-

mens examined for telomere length. Thus far, evidence of telomerase-negative clinical tumors having such long telomeres is not reported.

Few studies have comprehensively addressed the relationship between telomerase activity and prognosis. In neuroblastoma, high telomerase activity correlated with poor prognosis *(33)*. Similar findings are reported in gastric cancer *(35)* and breast cancer *(45)* but not in renal cell carcinomas *(37)*. In this series, NSCLCs having high telomerase activity had a more unfavorable prognosis than telomerase-negative tumors, but the differences were not statistically significant. While these data suggest that telomerase has a weak, or no, prognostic impact in lung cancer, perhaps the addition of more patients to this series and a longer follow-up would clarify the question of prognostic impact of telomerase activity in NSCLC. In this series, three patients with telomerase-negative primary NSCLC still relapsed despite surgical resection. Selection of telomerase-positive clones may eventually occur at distant metastatic sites when telomeres are critically shortened. It is reported in lung cancer that telomerase activation and telomere shortening at distant metastatic sites can occur when primary tumors are telomerase negative *(18)*. Since most patients with lung cancer succumb to distant disease, anti-telomerase treatments may have a therapeutic role in the prevention of metastasis after successful local control of the primary tumors *(9,46)*.

In many tumors, the mean telomere length, as estimated by TRF analysis, is similar to that found in the corresponding adjacent normal tissue *(33,34,41,47,48)*. In this study, the mean and peak TRF lengths in the tumors were often similar to those in the adjacent, benign lung tissue, although the values were occasionally either smaller or larger in the tumor. Altered TRF lengths are reported to be linked both to high telomerase activity *(33,34)* and to the lack of measurable telomerase activity *(37)*. In tumor-derived cell lines, no association was found between telomere length and telomerase activity *(18)*. As recently reported, telomere length alone is unlikely to be an accurate predictor of cellular immortality *(34)*.

Telomerase activity is linked to proliferation in diverse cellular contexts *(26,49)*. In quiescent, primitive, hematopoietic progenitor cells, basal telomerase levels are low, but the enzymatic activity is rapidly up-regulated when the cells are activated to enter the cell cycle following exposure to combinations of hematopoietic growth factors *(26)*. In certain human tumor cell lines, such as acute promyelocytic leukemia and human embryonal carcinoma cell lines, telomerase activity is repressed following induced differentiation in maturation-sensitive but not maturation-resistant cell lines *(22,50)*. Telomerase is also repressed in tumor cell lines when the cells become quiescent, as reported previously *(51,52)*. These observations indicate that telomerase activity and cellular proliferation may be linked in clinical tumors. In breast cancer, telomerase activity correlated with S-phase fraction in lymph node-positive breast cancer *(45)*, but other investigators *(32)* failed to find such an association. In this study, a high proliferation rate for tumor cells was associated with telomerase activity, suggesting that telomerase is activated in lung cancer when growth-stimulatory signals are triggered. The pattern of telomerase activity versus Ki-67 immunostaining shown in Fig. 2, B, indicates that tumor cell subpopulations may exist, since specimens with no or low telomerase activity were less correlated with proliferation rates than specimens with higher telomerase activity ($r = +.148$ for activity $\leq$10 TPG and $r = +.376$ for activity >10 TPG, plus data not shown).

In summary, high telomerase activity measured in primary NSCLC was found to be associated with an increased cellular proliferation index and advanced tumor stage. These findings indicate that telomerase activity may contribute to lung tumorigenesis and its progression. These observations support the concept of telomerase as an attractive therapeutic target in lung cancer.

References

(1) Blackburn EH. Structure and function of telomeres. Nature 1991;350:569–73.

(2) Greider CW, Blackburn EH. Identification of a specific telomere terminal transferase activity in *Tetrahymena* extracts. Cell 1985;43:405–13.

(3) Morin GB. The human telomere terminal transferase enzyme is a ribonucleoprotein that synthesizes TTAGGG repeats. Cell 1989;59:521–9.

(4) Allsopp RC, Vaziri H, Patterson C, Goldstein S, Younglai EV, Futcher AB, et al. Telomere length predicts replicative capacity of human fibroblasts. Proc Natl Acad Sci U S A 1992;89:10114–8.

(5) Vaziri H, Dragowska W, Allsopp RC, Thomas TE, Harley CB, Lansdorp PM. Evidence for a mitotic clock in human hematopoietic stem cells: loss of telomeric DNA with age. Proc Natl Acad Sci U S A 1994;91:9857–60.

(6) Harley CB, Futcher AB, Greider CW. Telomeres shorten during ageing of human fibroblasts. Nature 1990;345:458–60.

(7) Hastie ND, Dempster M, Dunlop MG, Thompson AM, Green DK, Allshire RC. Telomere reduction in human colorectal carcinoma and with ageing. Nature 1990;346:866–8.

(8) Kim NW, Piatyszek MA, Prowse KR, Harley CB, West MD, Ho PLC, et al. Specific association of human telomerase activity with immortal cells and cancer. Science 1994;226:2011–5.

(9) Harley CB, Kim NW, Prowse KR, Weinrich SL, Hirsch KS, West MD, et al. Telomerase, cell immortality, and cancer. Cold Spring Harbor Symp Quant Biol 1994;59:307–15.

(10) Counter CM, Botelho FM, Wang P, Harley CB, Bacchetti S. Stabilization of short telomeres and telomerase activity accompany immortalization of Epstein-Barr virus-transformed human B lymphocytes. J Virol 1994;68:3410–4.

(11) Counter CM, Hirte HW, Bacchetti S, Harley CB. Telomerase activity in human ovarian carcinoma. Proc Natl Acad Sci U S A 1994;91:2900–4.

(12) de Lange T. Activation of telomerase in a human tumor. Proc Natl Acad Sci U S A 1994;91:2882–5.

(13) Feng J, Funk WD, Wang SS, Weinrich SL, Avilion AA, Chiu C, et al. The RNA component of human telomerase. Science 1995;269:1236–41.

(14) Harrington L, McPhail T, Mar V, Zhou W, Oulton R, Bass MB, et al. A mammalian telomerase-associated protein. Science 1997;275:973–7.

(15) van Steensel B, de Lange T. Control of telomere length by the human telomeric protein TRF1. Nature 1997;385:740–3.

(16) Rusch V, Klimstra D, Venkatraman E, Pisters P, Langenfeld J, Dmitrovsky E. Overexpression of the EGFR and its ligand, TGFα, is frequent in resectable non-small cell lung cancer, but does not predict tumor progression. Clin Cancer Res 1997;3:515–22.

(17) Strauss GM, Kwiatkowski DJ, Harpole DH, Lynch TJ, Skarin AT, Sugarbaker DJ. Molecular and pathologic markers in stage I non-small-cell carcinoma of the lung. J Clin Oncol 1995;13:1265–79.

(18) Hiyama K, Hiyama E, Ishioka S, Yamakido M, Inai K, Gazdar AF, et al. Telomerase activity in small-cell and non-small-cell lung cancers. J Natl Cancer Inst 1995;87:895–902.

(19) Martini N, Flehinger BJ. The role of surgery in N2 lung cancer. Surg Clin North Am 1987;67:1037–49.

(20) Tisi GM, Friedman PJ, Peters RM, Pearson FG, Carr D, Lee RE, et al. Clinical staging of primary lung cancer. Am Rev Respir Dis 1983;127:659–64.

(21) Mountain CF. A new international staging sys-

tem for lung cancer. Chest 1986;89(4 Suppl): 225S–233S.
(22) Albanell J, Han W, Mellado B, Gunawardane R, Scher HI, Dmitrovsky E, et al. Telomerase activity is repressed during differentiation of maturation-sensitive but not resistant human tumor cell lines. Cancer Res 1996;56:1503–8.
(23) Piatyszek MA, Kim NW, Weinrich SL, Hiyama K, Hiyama E, Wright WE, et al. Detection of telomerase activity in human cells and tumors by a telomeric repeat amplification protocol (TRAP). Meth Cell Sci 1995;17:1–15.
(24) Wright WE, Shay JW, Piatyszek MA. Modifications of a telomeric repeat amplification protocol (TRAP) result in increased reliability, linearity and sensitivity. Nucleic Acids Res 1995; 23:3794–5.
(25) Cattoretti G, Becker MH, Key G, Duchrow M, Schluter C, Galle J, et al. Monoclonal antibodies against recombinant parts of the Ki-67 antigen (MIB 1 and MIB 3) detect proliferating cells in microwave-processed formalin-fixed paraffin sections. J Pathol 1992;168:357–63.
(26) Engelhardt M, Kumar R, Albanell J, Pettengell R, Han W, Moore MA. Telomerase regulation, cell cycle, and telomere stability in primitive hematopoietic cells. Blood 1997;90:182–93.
(27) Hollander M, Wolfe DA. Nonparametric statistical methods. New York: Wiley, 1973.
(28) Kaplan EL, Meier O. Nonparametric estimation from incomplete observations. Am Stat Assoc J 1958;53:457–81.
(29) Mantel N. Evaluation of survival data and two new rank order statistics arising in its consideration. Cancer Chemother Rep 1966;50: 163–70.
(30) Cox DR. Regression models and life tables [with discussion]. J R Stat Soc B 1972;34: 187–220.
(31) Rusch V, Klimstra D, Venkatraman E, Oliver J, Martini N, Gralla R, et al. Aberrant p53 expression predicts clinical resistance to cisplatin-based chemotherapy in locally advanced non-small cell lung cancer. Cancer Res 1995; 55:5038–42.
(32) Bednarek AK, Sahin A, Brenner AJ, Johnston DA, Aldaz CM. Analysis of telomerase activity levels in breast cancer: positive detection at the *in situ* breast carcinoma stage. Clin Cancer Res 1997;3:11–6.
(33) Hiyama E, Hiyama K, Yokoyama T, Matsuura Y, Piatyszek MA, Shay JW. Correlating telomerase activity levels with human neuroblastoma outcomes. Nature Med 1995;1:249–55.
(34) Hiyama E, Gollahon L, Kataoka T, Kuroi K, Yokoyama T, Gazdar AF, et al. Telomerase activity in human breast tumors. J Natl Cancer Inst 1996;88:116–22.
(35) Hiyama E, Yokoyama T, Tatsumoto N, Hiyama K, Imamura Y, Murakami Y, et al. Telomerase activity in gastric cancer. Cancer Res 1995;55: 3258–62.
(36) Counter CM, Gupta J, Harley CB, Leber B, Bacchetti S. Telomerase activity in normal leukocytes and in hematologic malignancies. Blood 1995;85:2315–20.
(37) Mehle C, Piatyszek MA, Ljungberg B, Shay JW, Roos G. Telomerase activity in human renal cell carcinoma. Oncogene 1996;13: 161–6.
(38) Sugino T, Yoshida K, Bolodeoku J, Tahara H, Buley I, Manek S, et al. Telomerase activity in human breast cancer and benign breast lesions: diagnostic applications in clinical specimens, including fine needle aspirates. Int J Cancer 1996;69:301–6.
(39) Kyo S, Kanaya T, Ishikawa H, Ueno H, Inoue M. Telomerase activity in gynecological tumors. Clin Cancer Res 1996;2:2023–8.
(40) Tahara H, Nakanishi T, Kitamoto M, Nakashio R, Shay JW, Tahara E, et al. Telomerase activity in human liver tissues: comparison between chronic liver disease and hepatocellular carcinomas. Cancer Res 1995;55:2734–6.
(41) Bacchetti S, Counter CM. Telomeres and telomerase in human cancer. Int J Oncol 1995; 7:423–32.
(42) Shay JW, Wright WE. Telomerase activity in human cancer. Curr Opin Oncol 1996;8: 66–71.
(43) Gupta J, Han LP, Wang P, Gallie BL, Bacchetti S. Development of retinoblastoma in the absence of telomerase activity. J Natl Cancer Inst 1996;88:1152–7.
(44) Bryan TM, Englezou A, Gupta J, Bacchetti S, Reddel RR. Telomere elongation in immortal human cells without detectable telomerase activity. EMBO J 1995;14:4240–8.
(45) Kim NW, Levitt D, Huang G, Wu F, Osborne K, Clark G. Correlation of telomerase with prognostic indicators of breast cancer [abstract]. Proc Am Assoc Cancer Res 1996;37: 561–2.
(46) Morin GB. Is telomerase a universal cancer target? [editorial]. J Natl Cancer Inst 1995;87: 859–61.
(47) Hiyama E, Yokoyama T, Hiyama K, Yamakido M, Santo T, Kodama T, et al. Alteration of telomeric repeat length in adult and childhood solid neoplasias. Int J Oncol 1995; 6:13–6.
(48) Hiyama K, Ishioka S, Shirotani Y, Inai K, Hiyama E, Murakami I, et al. Alterations in telomeric repeat length in lung cancer are associated with loss of heterozygosity in p53 and Rb. Oncogene 1995;10:937–44.
(49) Hiyama K, Hirai Y, Kyoizumi S, Akiyama M, Hiyama E, Piatyszek MA, et al. Activation of telomerase in human lymphocytes and hematopoietic progenitor cells. J Immunol 1995; 155:3711–5.
(50) Sharma HW, Sokoloski JA, Perez JR, Maltese JY, Sartorelli AC, Stein CA, et al. Differentiation of immortal cells inhibits telomerase activity. Proc Natl Acad Sci U S A 1995;92: 12343–6.
(51) Holt SE, Wright WE, Shay JW. Regulation of telomerase activity in immortal cell lines. Mol Cell Biol 1996;16:2932–9.
(52) Zhu X, Kumar R, Mandal M, Sharma N, Sharma HW, Dhingra U, et al. Cell cycle-dependent modulation of telomerase activity in tumor cells. Proc Natl Acad Sci U S A 1996; 93:6091–5.

Notes

Present address: J. Albanell, Oncology Service, Hospital Vall d'Hebron, Barcelona, Spain.

Supported by Public Health Service (PHS) grant U19CA67842-01 (M. A. S. Moore) and PHS training grants T32CA09512 and K12CA01712 (J. Langenfeld) from the National Cancer Institute, National Institutes of Health, Department of Health and Human Services; by the Gar Reichman Fund of the Cancer Research Institute (M. A. S. Moore); by FIS BAE96/5706 from the Fondo de Investigacion Sanitaria, Spain (J. Albanell); by CIRIT 1996BEAI200087 from the Comissio Interdepartmental per a la Recerca i Innovacio Technologica, Spain (J. Albanell); and by DFG 95/3191/1-1 from Deutsche Forschungsgemeinschaft, Germany (M. Engelhardt). Also supported in part by the Byrne Fund (M. A. S. Moore and E. Dmitrovsky) and the Oracle Chemoprevention Research Fund (E. Dmitrovsky).

We thank Dr. N. W. Kim (Geron Corporation, Menlo Park, CA) for providing the modified TRAP assay protocol prior to publication, Dr. K. MacKenzie (Memorial Sloan-Kettering Cancer Center, New York, NY) for her insightful discussions, Mr. Barry J. Nevins for expert assistance in the preparation of the manuscript, and Ms. Melody Owens for her expert assistance in data management.

Manuscript received March 20, 1997; revised June 6, 1997; accepted September 5, 1997.

Interferon Alfa Versus Chemotherapy for Chronic Myeloid Leukemia: a Meta-analysis of Seven Randomized Trials

*Chronic Myeloid Leukemia Trialists' Collaborative Group**

Background: **Several randomized clinical trials in chronic myeloid leukemia (CML) have reported better patient survival with interferon alfa (IFN α) than with standard chemotherapeutic agents, such as busulfan or hydroxyurea. However, the size and persistence of this survival benefit is uncertain. Our aim was to assess these reliably, both overall and in particular patient subgroups.** ***Methods:*** **We collaborated in a worldwide overview of all clinical trials in which patients with CML were randomly assigned to receive either IFN α as the main drug or standard chemotherapy. Trials were identified by electronic and hand searching of the medical literature and databases and by personal contact. Individual patient data were available for each of 1554 patients who had been randomly assigned to treatment in seven trials (German, Italian, British, French, Japanese, and ''Benelux''). Intention-to-treat stratified logrank survival analyses were performed, reporting two-sided *P* values.** ***Results:*** **Almost all of the patients in these trials had disease with the Philadelphia chromosome abnormality. Among those who did, the regimens that involved IFN α produced a statistically significantly better survival than those involving either hydroxyurea (*P* = .001) or busulfan (*P* = .00007) alone. The 5-year survival rates were 57% with IFN α and 42% with chemotherapy, with an absolute difference of 15% (standard deviation = 3%; *P*<.00001). There were no trials or subgroups of patients in which the treatment difference was statistically significantly different from the average.** ***Conclusion:*** **For patients with Philadelphia chromosome-positive chronic myeloid leukemia, the inclusion of IFN α in the therapeutic regimen produced substantially better 5-year survival than standard chemotherapy alone. [J Natl Cancer Inst 1997;89:1616–20]**

Chronic myeloid leukemia (CML) is a hematopoietic stem cell disorder that generally progresses, after some years of treatment, from a relatively benign chronic phase to an acute aggressive stage (blast crisis). Most patients diagnosed as having CML have leukemic cells with the Philadelphia (Ph) chromosome, in which a translocation between chromosomes 9 and 22 has resulted in the fusion of the BCR and ABL genes (which encode a serine-threonine kinase and a tyrosine kinase, respectively) to form an oncogene *(1)*. This definite chromosomal abnormality allows reduction of the population of leukemic cells to be monitored, and interferon alfa (IFN α) can cause at least temporary disappearance of the disease, as monitored by basic cytogenetics, in some patients.

Since the introduction of IFN α for the treatment of CML, several randomized clinical trials have reported significantly better survival for patients treated with this biologic response modifier than for patients treated with standard chemotherapeutic agents, such as busulfan or hydroxyurea *(2–5)*. To assess reliably the size and persistence of any survival benefit and to establish whether there is a particularly large or small benefit in various subgroups, a worldwide collaborative overview of the randomized evidence has been conducted. This form of analysis has two advantages; it avoids selective overemphasis on the results of particular studies and, because large numbers are involved, it reduces the effects of the play of chance. The aim of this collaboration was to assess the difference in survival of patients when IFN α is compared with standard chemotherapy and to establish whether any such difference is greater in particular types of patient.

Materials and Methods

Randomized trials of CML treatment were sought that began before 1990 and compared IFN α with chemotherapy—that is, versus busulfan, versus hydroxyurea or, in a three-way randomization, versus both. (These three-way trials also provided directly randomized comparisons of busulfan versus hydroxyurea, since they involved randomization to three treatment groups: IFN α versus busulfan versus hydroxyurea.) Medline and computerized clinical trial databases were searched; meeting abstracts, reference lists, and review articles were examined; and experts and pharmaceutical companies were contacted *(6)*. Once a relevant trial had been identified, information, including the most recent follow-up available, was sought on each randomized patient. This information included sex, Ph chromosome positivity, platelet and white blood cell counts, and Sokal score at diagnosis, along with dates of birth, diagnosis, and randomization. The follow-up variables collected included date last seen alive, date and type of response, date and type of any bone marrow transplant, and date and cause of death. These data were checked centrally for any obvious inconsistencies (e.g., dates out of order), for balance between treatments within different subgroups and over time, and for apparent discrepancies with any publications. As far as possible, data were to be obtained for all patients who had ever been randomized, irrespective of whether they had been included in previously published trial analyses. Tabulations of their own data (listing the numbers randomized and the numbers of deaths in various subgroups) were sent to the trialists for checking, thereby ensuring that the data had been correctly interpreted. The methods for this type of meta-analysis (i.e., based on individual patient data) have been described in detail elsewhere *(6)*.

Some trials allowed random assignment of Ph-negative patients, but the main analyses involve only the Ph-positive patients. Since the number of patients not known to be Ph positive was small, however, their inclusion or exclusion has no material effect on the overall result.

Statistical Analysis

Intention-to-treat analyses were used, with patients compared on the basis of their randomly allocated treatment, regardless of whether it was actually received. Logrank survival analyses for each trial yielded, for the IFN α-allocated group, the observed number of deaths (O), the expected number of deaths (E), and the variance (V) of the difference between these values for each trial (O–E). These were then summed, one per trial, and used to calculate the death rate ratio [by the ''one-step'' approximation exp[(O–E)/V] to the hazard function ratio *(7,8)*]. These death rate ratios are sometimes described in terms of percentage odds reductions: thus, for example, a ratio of 0.70 with standard deviation (SD) 0.06 could be described as a reduction of 30% (SD = 6%) in the annual death rate. All *P* values quoted are two-sided. For trials that involved 2:1 (or 1:2) randomization, the logrank tests are calculated in the usual way *(7)*, but, to balance the contribution from each randomization between the two treatment arms, the chemotherapy group counts twice (or half) just in the crude subtotals of deaths and patients.

Trials Included

Table 1 shows the 11 trials that were identified. Data were available for seven of them. The missing

**Correspondence to:* CML Trialists' Collaborative Group, Clinical Trial Service Unit, Radcliffe Infirmary, Oxford OX2 6HE, U.K.

See ''Notes'' following ''References.''

Table 1. List of all relevant randomized trials that began before 1990: interferon alfa (IFN α) versus busulfan or hydroxyurea*

Study (reference No.)	Induction treatment	IFN α dose	IFN α target WBC	Additional therapy if necessary	Alternative treatment	Chemotherapy target WBC	Ph-negative patients eligible	No. of		Median years follow-up of survivors
								Patients	Deaths	
Trials that are available										
Italian-CML-86 *(2)*	IFN α	9 MU/d		HU or Bu if WBC >30	HU	<30	No	322	198	9
German-CML-1 *(3)*	IFN α	5 MU/m^2/d	2–4	nil	Bu HU	<20 5–15	Yes	603	329	3
MRC-CML-3 *(4)*	Chemo-therapy	3 MU/d	2–5	HU or Bu if WBC >30	Bu HU	4–20 or <30 4–20	Yes	590	331	4
Benelux *(9)*	Chemo-therapy	3 MU × 5/w	<10	HU to keep WBC <10	HU	<10	No	197	72	4
Pessac *(10)*	IFN α	4 MU/m^2/d		nil	HU	4–10	Yes	22	10	6
EORTC-06887	Chemo-therapy	5 MU/d	<10	A-BMT if complete cytogenetic response	HU	<15	Yes	78	20	2
Japan *(5)*	IFN α	9 MU/d	5	nil	Bu	5	No	170	60	4
Trials that are not available										
Washing-ton *(11)*	IFN α	4 MU/m^2/d			HU			18		
Schering-plough	IFN α	4 MU/m^2/d	<15		HU	4–10		133		
MEX-INC-CML	IFN α	5 MU/m^2/d	<20		Bu	<20		30		
Castilla-Leon *(12)*	Chemo-therapy	2 MU/d	<10	HU to keep WBC <10	HU	5–10		26		

*HU = hydroxyurea, Bu = busulfan, A-BMT = autologous bone marrow transplant, MU/m^2/d = mega-units of interferon/square meter/day, WBC = white blood cell count (in units of 10^9/L); note that in some trials Ph-negative patients were not eligible.

trials were small, however, so in total about 90% of the patients in these 11 trials have been included.

In the British Medical Research Council (MRC) CML-3 (MRC-CML-3) trial, patients were induced with busulfan or with hydroxyurea (selected either by randomization or, often, by physician choice) and were randomized to receive IFN α or to continue with the treatment that had been used for induction. This trial was therefore split into two, one part comparing IFN α versus busulfan and the other comparing IFN α versus hydroxyurea.

The German CML-1 trial began as a 1:1 randomization between busulfan and hydroxyurea, with IFN α introduced as a third arm for most centers in 1986 (initially in the ratio 1:1:1 and later in the ratio 1:1:2). In this report, these three parts of the study are analyzed separately and the results then summed. Only the second and third parts contribute directly to the comparison of IFN α versus busulfan, of IFN α versus hydroxyurea, or (by logrank analyses that avoid any double counting) of IFN α versus chemotherapy (either busulfan or hydroxyurea) (Fig. 1).

Results

IFN α Versus Chemotherapy

Fig. 1 shows the results among Ph-positive patients for each separate trial. There is an overall reduction in the annual death rate of 30% (SD = 6%), which is highly statistically significant (P<.00001). Confidence intervals for each of the trials overlap this average reduction, indicating that no trial had a result that was statistically significantly different from the average, and a formal test for heterogeneity between the different trial results was likewise not statistically significant. Some patients received a bone marrow transplant in chronic phase, but censoring at transplant makes no material difference to the results, giving an overall reduction in the annual death rate of 32% (SD = 7%).

The overall reduction in the annual death rate is 26% (SD = 8%; P = .001) in the trials of IFN α against hydroxyurea, and 36% (SD = 9%; P = .00007) in the trials of IFN α against busulfan. Although the comparison of IFN α versus busulfan yields a somewhat greater reduction, this result is not significantly different from the result yielded by the comparison of IFN α versus hydroxyurea. Fig. 2 shows the cumulative effect on survival. Median survival is prolonged by about 1 or 2 years and there is an improvement in the 5-year survival rates from 42% with chemotherapy to 57% with IFN α, an absolute difference of 15% (SD = 3%; with logrank P<.00001). The absolute improvement in the 5-year survival rate is 20% (SD = 5%) in the trials of IFN α versus busulfan and 12% (SD = 4%) in the trials of IFN α versus hydroxyurea.

For Ph-positive patients, analyses within Sokal stage *(13)*, age, and sex groups did not reveal any heterogeneity between the sizes of the effects in any of these subgroups (Fig. 3). The analyses among Ph-negative and Ph-unknown patients are shown separately in Fig. 3, but there were too few such patients for these results to be informative.

The results in different time periods are given separately in Fig. 3. Throughout the first 5 years, the annual death rate was lower in those allocated IFN α than in those allocated chemotherapy, but after 5 years it appears not to be. This does not, however, suggest that the benefit accrued during the first 5 years is then lost. It merely suggests that, among those who do survive to 5 years (which will be a greater proportion of one group than of the other; Fig. 2), the subsequent prognosis is about the same in both groups. Thus, the crude mortality during the first 5 years is 312 of 864 for the IFN α patients versus 415 of 830 for the adjusted control group (i.e., 36% versus 50%, corresponding to an absolute difference of 14%, which is similar to the absolute difference of 15% in the 5-year survival in Fig. 2). The numbers still alive and being followed at the end of the first 5 years were 254 for the IFN α patients versus 185 for the adjusted con-

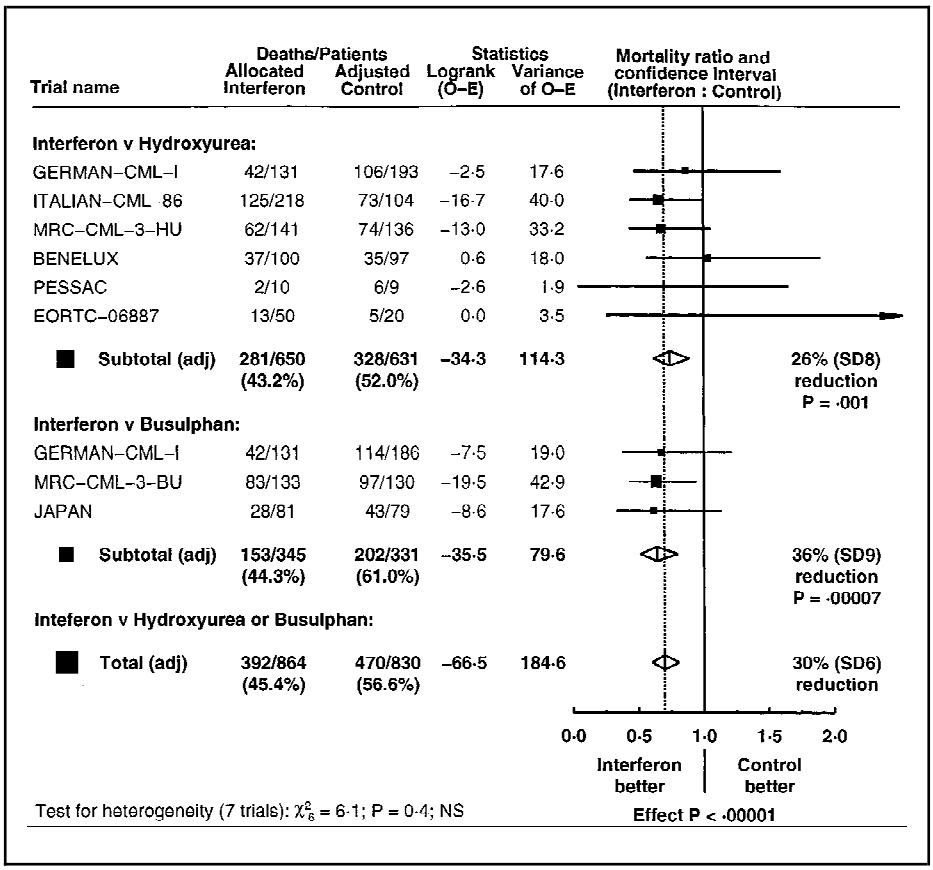

Fig. 1. Ratios of annual death rates in the randomized trials of interferon alfa (IFN α) versus control (hydroxyurea or busulfan) in Philadelphia chromosome-positive chronic myeloid leukemia (CML): combination of evidence from different trials. Each trial result is represented by a square, with larger squares for trials with more data and a horizontal line indicating the 99% confidence interval (CI). Squares to the left of the solid vertical line indicate better results with IFN α, but if the CI crosses this line, the result is not significant at the $P = .01$ level. Subtotals and the overall result are represented by diamonds whose widths show the 95% CIs, accompanied by the percentage odds reduction and its standard deviation (SD). Note: Where a trial had several parts, with separate randomization procedures, each part is analyzed separately and the results of these analyses are added together. Where randomization was in a 2:1 (or 1:2) ratio, twice (or half) the numbers of deaths and patients in the chemotherapy arm are added into the adjusted (adj) total to balance the contribution from each study, but this adjustment does not affect the calculation of the logrank observed minus expected (O–E) or its variance. The German trial was in three parts in which the hydroxyurea:busulfan:IFN α allocation ratios differed, being (i) 1:1:0 (with 71 deaths of 105 to allocated hydroxyurea and 72 deaths of 109 to allocated busulfan); (ii) 1:1:1 (with mortality 13 of 35:22 of 32:12 of 27, respectively); and (iii) 1:1:2 (with mortality 22 of 53:20 of 45:30 of 104, respectively). Although there are 510 patients in parts i, ii, and iii, only the 296 patients in parts ii and iii provide directly randomized comparisons between IFN α and chemotherapy. (The logrank O–E and its variance for IFN α versus chemotherapy were −0.8 and 9.3 in part ii and −6.3 and 17.9 in part iii.)

trol group. The crude death rate among them after the first 5 years was 80 of 254 for the IFN α patients versus 55 of 185 for the adjusted control group (31% versus 30%), indicating no further difference. However, since 85% of the deaths thus far reported in these trials occurred during the first 5 years, the evidence on what happens later is limited, as may be seen from the wide 99% confidence interval for the final black square in Fig. 3.

Hydroxyurea Versus Busulfan

The three-way comparison in the German CML-I trial *(14)* and the induction randomization in the MRC-CML-3 trial *(4)* also provide some limited evidence on hydroxyurea versus busulfan. In these two trials, hydroxyurea appeared to be the better option. In comparison with allocation to busulfan, allocation to hydroxyurea reduced the proportional odds of death by 24% (SD = 10%; $P = .02$), suggesting an absolute improvement in the 5-year survival rate of about 10% but with wide confidence intervals. Again, analyses within Sokal stage, age, sex, and Ph status groups did not show any statistically significant heterogeneity between the effects in different subgroups (data not shown), but the numbers randomized between these two chemotherapy agents are too small for such subgroup analyses to be reliable.

Discussion

For patients with Ph-positive CML, these seven randomized trials that compared IFN α (as the main drug) versus continued chemotherapy demonstrate a highly statistically significant survival benefit for the regimens that involved IFN α, with an absolute improvement in 5-year survival of 15% (SD = 3%) from 42% to 57%. This estimate may be somewhat reduced, due to the inclusion in some trials of patients who were not in early chronic phase. The majority of patients with CML are over the age of 60 years, and since repeated injections of IFN α can involve considerable inconvenience, costs, and side effects *(2,3,5)*, it would be useful to know whether there are some recognizable types of patient who can expect little benefit. Unfortunately, however, this cannot be determined reliably from these trials.

A larger treatment effect in the Sokal stage 1 subgroup was reported in the MRC CML-3 trial *(4)*, but this is not confirmed in the overview. There was no statistically significant evidence of any different treatment effect in any particular sex, age, or risk group, although the possibility that IFN α is more beneficial in some groups than others cannot be excluded. The number of patients randomized who were not Ph positive was too small to be informative. It is possible that the size of benefit obtained with IFN α varies according to the degree and time of hematologic and cytogenetic response. However, the information available from these trials is not sufficient to investigate this properly. If chemotherapy is to be used, hydroxyurea appears better than busulfan, but regimens that involve IFN α result in statistically significantly better 5-year survival than those involving either chemotherapeutic agent. There was no statistically significant heterogeneity of treatment effect between these trials, even though they used a variety of different treatment policies, but this does not preclude the possibility that some policies are better than others. In particular, it is not yet clear what the dosage or duration

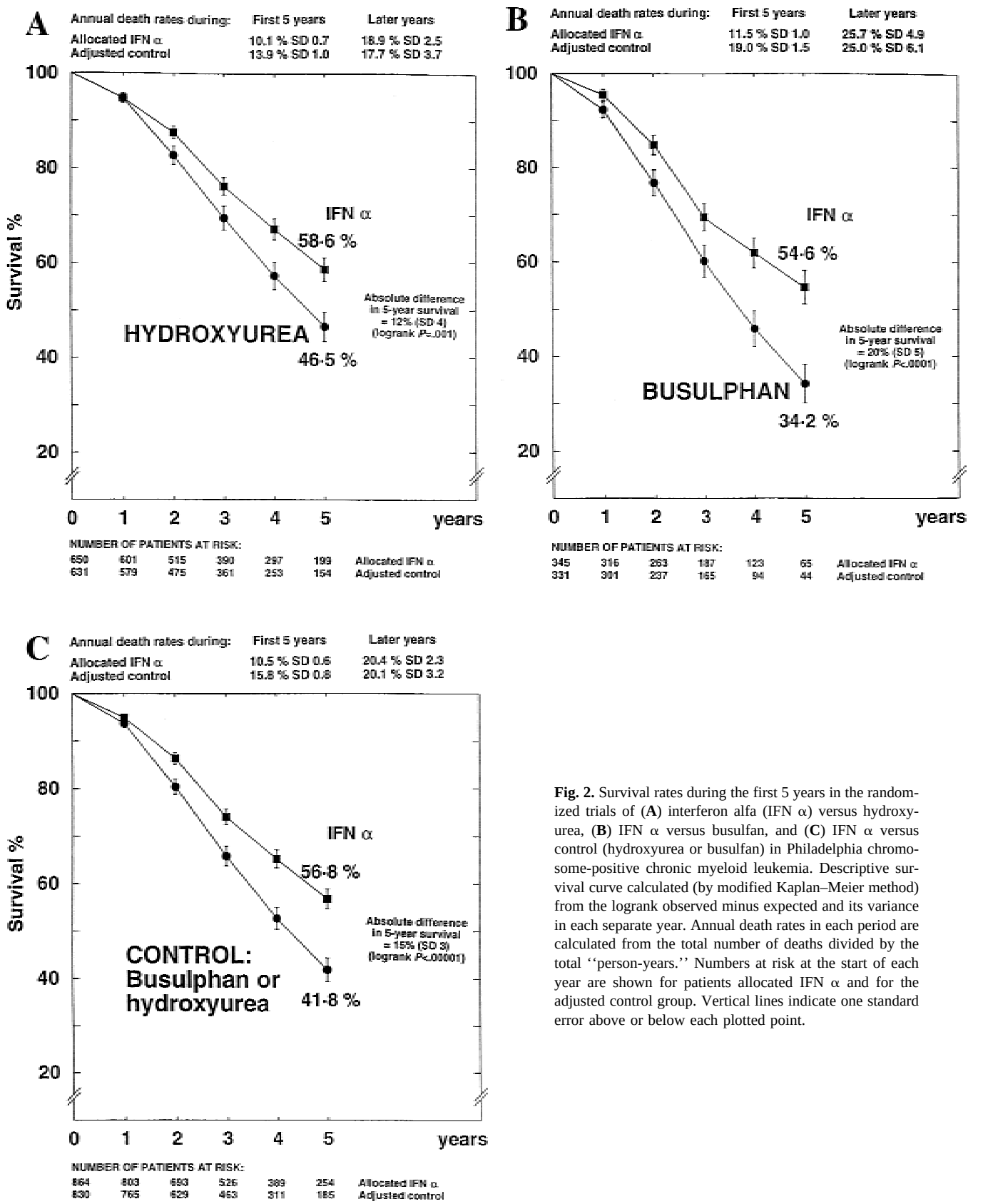

Fig. 2. Survival rates during the first 5 years in the randomized trials of (**A**) interferon alfa (IFN α) versus hydroxyurea, (**B**) IFN α versus busulfan, and (**C**) IFN α versus control (hydroxyurea or busulfan) in Philadelphia chromosome-positive chronic myeloid leukemia. Descriptive survival curve calculated (by modified Kaplan–Meier method) from the logrank observed minus expected and its variance in each separate year. Annual death rates in each period are calculated from the total number of deaths divided by the total ''person-years.'' Numbers at risk at the start of each year are shown for patients allocated IFN α and for the adjusted control group. Vertical lines indicate one standard error above or below each plotted point.

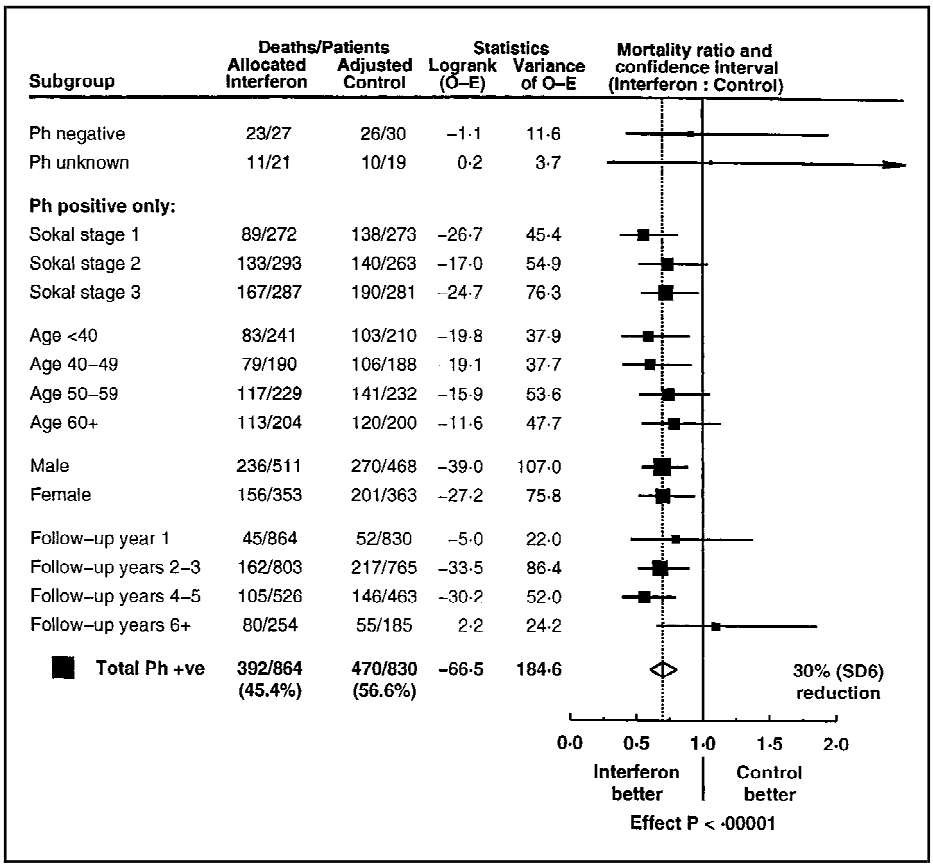

Fig. 3. Ratios of annual death rates in the randomized trials of interferon alfa (IFN α) versus control (hydroxyurea or busulfan) in chronic myeloid leukemia, subdivided by patient characteristics and years since randomization. Ph = Philadelphia chromosome; SD = standard deviation; and O–E = logrank observed minus expected. No statistically significant heterogeneity of effect was found with respect to any of these factors.

of IFN α should be or how best to combine IFN α with chemotherapy.

References

(1) Gordon MY, Goldman JM. Cellular and molecular mechanisms in chronic myeloid leukaemia: biology and treatment. Br J Haematol 1996;95:10–20.

(2) Interferon alfa-2a as compared with conventional chemotherapy for the treatment of chronic myeloid leukemia. The Italian Cooperative Study Group on Chronic Myeloid Leukemia. N Engl J Med 1994;330:820–5.

(3) Hehlmann R, Heimpel H, Hasford J, Kolb HJ, Pralle H, Hossfield DK, et al. Randomized comparison of interferon-alpha with busulfan and hydroxyurea in chronic myelogenous leukemia. Blood 1994;84:4064–77.

(4) Allan NC, Richards SM, Shepherd PC. UK Medical Research Council randomised, multicentre trial of interferon-alfa n1 for chronic myeloid leukaemia: improved survival irrespective of cytogenetic response. The UK Medical Research Council's Working Parties for Therapeutic Trials in Adult Leukemia. Lancet 1995;345:1392–7.

(5) Ohnishi K, Ohno R, Tomonaga M, Kamada N, Onozawa K, Kuramoto A, et al. A randomized trial comparing interferon-alpha with busulfan for newly diagnosed chronic myelogenous leukemia in chronic phase. Blood 1995;86: 906–16.

(6) Stewart LA, Clarke MJ. Practical methodology of meta-analyses (overviews) using updated individual patient data. Cochrane Working Group. Stat Med 1995;14:2057–79.

(7) Early Breast Cancer Trialists' Collaborative Group. Systemic treatment of early breast cancer by hormonal, cytotoxic, or immune therapy. 133 randomised trials involving 31,000 recurrences and 24,000 deaths among 75,000 women. Early Breast Cancer Trialists' Collaborative Group. Lancet 1992;339: 1–15.

(8) Secondary prevention of vascular disease by prolonged antiplatelet treatment. Antiplatelet Trialists' Collaboration. Br Med J 1988;296:320–31.

(9) Low-dose interferon-alpha 2b combined with hydroxyurea versus hydroxyurea alone for chronic myelogenous leukemia. The Benelux CML Study Group. Bone Marrow Transplant 1996;17(Suppl 3):s19–s20.

(10) Broustet A, Reiffers J, Marit G, Fiere D, Jaubert J, Reynaud J, et al. Hydroxyurea versus interferon alfa-2b in chronic myelogenous leukaemia: preliminary results of an open French multicentre randomized study. Eur J Cancer 1991;27(Suppl 4):s18–s21.

(11) Jacobson RJ, St. Germain D. Reduced toxicities using interferon-alfa (IFN) and hydroxyurea in chronic myelogenous leukemia (CML). ECCO meeting abstracts 1991;6:s254.

(12) Moro MJ, Gil S, Canizo C, Clemente J Fernandez, Guerras L, Fisac RM, et al. The treatment of chronic myelogenous leukemia with interferon alfa-2b plus hydroxyurea versus hydroxyurea alone. Haematologica 1991;76(Suppl 4):117.

(13) Sokal JE, Cox EB, Baccarani MI, Tura S, Gomez GA, Robertson JE, et al. Prognostic discrimination in ''good-risk'' chronic granulocytic leukemia. Blood 1984;63:789–99.

(14) Hehlmann R, Heimpel H, Hasford J, Kolb HJ, Pralle H, Hossfield DK, et al. Randomized comparison of busulfan and hydroxyurea in chronic myelogenous leukemia: prolongation of survival by hydroxyurea. The German CML Study Group. Blood 1993;82:398–407.

Notes

Supported by the Imperial Cancer Research Fund, the Medical Research Council, and the Biomed program of the European Union (grant PL-931247).

The groups and trialists who collaborated are listed alphabetically as follows: Benelux Chronic Myeloid Leukemia (CML) Study Group, Belgium and The Netherlands (A. Delannoy, J. C. Kluin-Nelemans, and A. Louwagie); EORTC, Leukaemia Cooperative Group (P. Stryckmanns and S. Suciu); German CML Study Group (R. Hehlmann, H. Heimpel, and J. Hasford); Italian Cooperative Study Group on CML (E. Zuffa, M. Baccarani, and S. Tura); Japan Kouseisho Leukemia Study Group (K. Ohnishi, R. Ohno); Medical Research Council, U.K. (N. Allan and P. Shepherd); and Pessac, France (A. Broustet). Secretariat (R. Alison, M. Clarke, H. Duong, R. Gray, E. Greaves, R. Peto, S. Richards, D. Sinclair, and K. Wheatley). Writing Committee (S. Richards, N. Allan, M. Clarke, R. Gray, and R. Peto).

Manuscript received December 16, 1996; revised May 29, 1997; accepted August 28, 1997.